

**INVESTIGATION OF WIND CHARACTERISTICS AND ESTIMATION OF
WIND POWER POTENTIAL OF NAROK COUNTY USING WEIBULL AND
WAVELET TECHNIQUES.**

OKOTH STEVEN OCHOLA

**Research thesis submitted in partial fulfilment of the requirements for the award of
master of science degree in physics of Maasai Mara University**

2024

Declaration

I hereby declare that this thesis is my original work and has never been presented anywhere for academic or any other purpose as it may be. Due recognition and citation have been made where other peoples' work have been used.

Signature..... Date.....

OKOTH STEVEN OCHOLA

SM03/JP/MN/13771/2021

SUPERVISORS

We hereby confirm that this is the candidate's original work under our supervision.

1. DR. OTIENO FREDRICK

Signature.....

Date.....

2. DR. ISAAC MOTOCHI

Signature.....

Date.....

Dedication

I dedicate this research to my siblings Sonia Achola, Jephthers Achola and Maxwell Achola. I hope one day you will join me in the quest of unlocking the secrets of the universe through Physics or other science of your choice.

Abstract

Low exploitation of wind power in Kenya can be linked to the limited or nonexistent information on wind characteristics for many regions. This study aimed to address this gap by examining wind characteristics through Weibull and Wavelet techniques, evaluating both temporal, spatial, and spectral aspects to estimate wind power potential. Wavelet technique was used to study spectral characteristics while Weibull was used in fitting the wind data to obtain other temporal characteristics of the wind regime. Wind data of Narok county, recorded between 2011 and 2021 for Narok weather station, was analyzed using the Weibull and Wavelet techniques to avail the desired wind characteristics. The wind regime was characterized by an annual mean wind speed of 4.3 m/s which correspond to a mean wind power density of 126 W/m². Based on wind speed, wind regime in Narok can be classified as gentle breeze at 10 m. Based on wind power density, wind regime in Narok belongs to a class 2 wind power. The wind regime was found to have period of about 1 year and is dominated by frequencies in the range 0.4 Hz to 0.5 Hz. The wind predominantly blows from the East direction. Weibull distribution describes the wind regime in Narok with an accuracy of 0.94 based on R² error approximation technique which imply that Weibull distribution is about 94% accurate in describing the wind regime of Narok. The study found that wind regime in Narok was generally viable for wind power extraction at heights above 19 m regardless of the scale of wind power extraction.

Acknowledgements

My eternal gratitude goes to Almighty God; my Father, all time friend and ever faithful ally who's been always there by my side all through, even the most-scary parts of the journey when no one could. Indeed, this far, the Lord has brought me and I can never be grateful enough. My sincere gratitude goes to my supervisors, Dr. Otieno Fredrick and Dr. Motochi Isaac for their unwavering support throughout the entire research. Their unreserved guidance and pieces of advice proved vital to me during the entire journey. I would have made several mistakes along the way that would have been detrimental to my career if it were not for the guidance of the two supervisors. I did not only benefit academically but I also learnt several life lessons that I would carry with me my entire life. Am much wiser because of these two people; may God's abundant blessings be your portion. Special appreciations go to the Kenya Meteorological Department for availing the historical data that was used in the research.

I would like to thank the Maasai Mara university management for the conducive learning environment that enabled me to conduct the research successfully. Special gratitude also goes to the faculty members in the school of Pure, Applied and Health Sciences for the technical advice they offered. I would like to specifically mention Dr. Jared Ombiro, Dr. Duke Oeba, Prof. Justus Simiyu and Mr. Geoffrey Mwendwa for their insightful comments and massive support during the research. Your support meant a lot to me. I would like to specially thank the physics laboratory technologists; Mr. Eliud Yego and Mr. Aluko Sankara for granting me a place to sit and work during the research.

My eternal gratitude goes to my beloved parents, Mr. Henry Achola and Mrs. Everlyne Achola who have felt the greatest weight of my education in one way or another. Thank you for every inch of support that you accorded me.; I am forever indebted to you as my best friends. I would like to thank two special ladies in my life, Miss. Ellen Oyieko my fiancée and Miss Sonia Achola my youngest sibling for their love and prayers throughout the process. They made things bearable during tough times, may God bless you ladies for me. I will not forget my two other siblings, Maxwell Achola and Jephthers Achola who gave me a sense of responsibility and direction. May God reward you for your enormous support. To my Aunt Loyce, thank you for the sacrifices you made for me. May God bless your big heart. My two grandmas, both paternal and maternal sides, you have been the reason why I kept pushing even when I had every reason to give up. May God bless you for the love and encouragements.

Lastly, may I thank my colleagues; Dorothy Lwambe, Osoro Brian and Sammuel Muthini for the insightful discussions we had together. They were very helpful in my research. Sincere gratitude goes to Bro. Peter Nyangeresi, Kennedy Ogolla, Elder Joram Ouko, Ellen Oyieko, Reagan Odoyo and the entire Seventh Day Adventist Maasai Mara University fraternity for their unceasing prayers to God concerning the success of this research. They held my hands in prayers in their secret chambers and their prayers were indeed answered by God. May God bless you in all perspectives, I will forever be indebted. May God bless every single person mentioned here or anybody who assisted me in anyway during the research and have not been mentioned due to human limitations, you will forever have special place in my heart.

Table of Contents

Declaration	i
Dedication	ii
Abstract	iii
Acknowledgements	iv
List of figures	x
List of tables	xii
Flowchart symbols used with their corresponding meaning	xiv
CHAPTER ONE	1
INTRODUCTION	1
1.0 INTRODUCTION	1
1.1 Wind energy resource	3
1.2 Weibull probability distribution function	5
1.3 Morlet wavelet decomposition	6
1.6 JUSTIFICATION	9
1.7 GENERAL OBJECTIVE	10
1.8 SPECIFIC OBJECTIVES	10
CHAPTER TWO	11
LITERATURE REVIEW	11
2.0 Introduction	11

2.1 Why the study area was chosen	11
2.2 Review of available wind data analysis tools.....	14
2.2.0 Estimation of wind power potential using a mixture of PDFs.....	15
2.2.1 Homogeneous mixture PDF used in WPD estimation	15
2.2.2 Heterogenous mixture distribution used in WPD estimation.....	17
2.2.3 Estimation of wind power potential using One component (persistence) PDFs ...	19
2.3 Parameter estimation methods	22
2.4 Performance indicators	22
2.5 Continuous Wavelet Transform (CWT) as applied to wind data	23
CHAPTER THREE.....	25
METHODS	25
3.0 Introduction.....	25
3.1 Data Acquisition and Filtering	25
3.2 Wind direction determination	29
3.3 Mean wind speed and standard deviation	30
3.4 Wind speed variability with a hub height.....	31
3.6 Turbulence intensity variation	32
3.7 Weibull parameters	32
3.8 Measured and estimated Weibull densities	34
3.9 Wind speed carrying maximum energy and most probable wind speeds	34

3.10 Wind power densities	35
3.11 Wind speed spectral analysis using CWT	35
3.12 Error approximations (PDF performance analysis)	36
CHAPTER FOUR.....	37
RESULTS AND DISCUSSIONS	37
4.0 Introduction.....	37
4.1 Wind direction	37
4.2 Mean wind speeds and standard deviation	39
4.3 Mean wind speed variation with height.....	42
4.4 Wind turbulence intensity and wind turbine stalling time	44
4.5 Weibull parameters	47
4.6 Most probable wind speed and wind speed carrying maximum energy	50
4.7 Measured and estimated wind speed probability and cumulative distribution densities.....	51
4.8 Evaluation of Weibull fitness in fitting the wind regime.....	53
4.8 Wind speed frequency spectrum	53
4.9 Wind Power Density	57
CHAPTER FIVE	64
Conclusions and Recommendations	64
5.1 Conclusions.....	64

5.2 Recommendations	64
5.3 Appendices	65
References	73

List of figures

Figure 1:Kenya wind speed map as released by EPRA as of December 2019 [15].	4
Figure 2: Snapshot illustrating how matrices A, WD, B, C and D were made.....	27
Figure 3: Polar chart demonstrating wind directions over different wind speed ranges for Narok weather station.	37
Figure 4: Diurnal mean wind speed variation for Narok weather station.....	39
Figure 5: Mean wind speed variation over the months of the year for Narok weather station.....	41
Figure 6: Mean wind variation with respect to hub height for Narok weather station	43
Figure 7: Wind turbulence intensity over the hours of the day for Narok weather station.....	45
Figure 8: Turbulence intensity evolution over the year for Narok weather station.	46
Figure 9: Most probable wind speed and wind speed carrying maximum energy for Narok weather station.....	50
Figure 10: Mean wind speed probability distribution for Narok weather station.....	51
Figure 11: Mean wind speed cumulative probability distribution for Narok weather station.....	52
Figure 12: Time-frequency characteristics of the wind regime in Narok weather station displayed in a spectrogram.	53
Figure 13: Time-frequency characteristics of the wind regime in Narok weather station displayed in a spectrogram (divisions of Figure 12)	55
Figure 14: Time-frequency characteristics of the wind regime in Narok weather station displayed in a spectrogram, this a zoom in on region a of figure 13.	56
Figure 15: Mean wind power density over the months of the year for Narok weather station at 10 m height.....	57
Figure 16: Wind power density variation with height extrapolated from 10 m to 100 m height.	59

Figure 17: Comparison of the most probable, mean and maximum power densities over the year for Narok weather station at 10 m.....	61
Figure 18: Comparison of the actual mean wind power densities and approximated wind power densities calculated from averaging the maximum and most-probable wind power densities.....	61
Figure 19: Sub-plots of Figure 17	62
Figure 20: Flowchart for filtering wind speed data part I.....	65
Figure 21: Flowchart for filtering wind speed data part II.....	66
Figure 22: Flowchart for filtering wind direction data part I.....	67
Figure 23: Flowchart for filtering wind direction data part II	67
Figure 24: Flowchart showing the logic for tabulating WSD & WDD and plotting polar chart ..	68
Figure 25: Flowchart for determining hourly mean wind speed and standard deviation	69
Figure 26: Flowchart for calculating monthly and annual mean wind speed and standard deviation	70
Figure 27: Flowchart for calculating algorithm parameters k and c.....	71
Figure 28: Flowchart showing steps for computing estimated and measured probability and cumulative densities of Weibull distribution.	71
Figure 29: Flowchart showing the algorithm that was used for spectral analysis of WSD	72

List of tables

Table 1: Share of energy generation in Kenya as of the year 2022 [12].....	2
Table 2: Illustration of how the frequency distribution of the wind direction verses wind speed was done.....	29
Table 3: Weibull Parameters c and k over the months of the year at 10 m height	49

List of Symbols and Abbreviations

Γ : Gamma function .

$\psi_{a,b}(t)$: stand for the real part of the mother wavelet transform (morlet)

σ : standard deviation (m/s).

ω : Fundamental wavelet frequency.

c : Weibull scale parameters (m/s).

CWT: Continuous wavelet transforms.

$f(v, k, c)$: Weibull probability density function.

$F(v, k, c,)$: Weibull cumulative probability density function.

k : Weibull shape parameter (dimensionless)

N: Number of observations

PDF: Probability distribution function

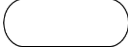

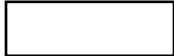

\bar{v} : mean wind speed (m/s):

v_i : wind speed (m/s).

WPD: Wind power density

$x(t)$: Original signal in study

Flowchart symbols used with their corresponding meaning

Flowchart symbol	Meaning
	Start/end of process
	Input/output of data symbol
	Data processing (e.g. calculation)
	Flowchart connector.
i, j	Are dummy symbols which may represent counters or values of data in a cell with an array
!= , ==	Not equal to, equal to respectively.
<, >	Less than, greater than respectively
mm/dd/yy	Month, day, year date
WSD/WS	Wind speed data
Stdv	Standard deviation
WD/WDD	Wind direction data
Del, cal, freq-dist-table	Delete, calculate, frequency distribution table

CHAPTER ONE

INTRODUCTION

1.0 INTRODUCTION

Global energy demand is steadily increasing, with the International Energy Agency (IEA) projecting a rise from the current 25,000 TWh to approximately 37,500-50,000TWh by 2050 (Agency, 2021). This surge is primarily driven by rapid population growth and urbanization. In Africa, energy demand is also rising quickly. The African Union Development Agency (AUDA) estimates that the continent's energy needs will more than triple by 2050, which is significantly higher than the global average. This notable increase is due to Africa having the fastest-growing population and ongoing development. Currently, energy consumption in Africa shows that biomass represents 45%, crude oil 23%, coal 13%, natural gas 16%, and renewables just 2% (kfw et al., 2021). Similarly, in the East Africa Community (EAC) region, biomass accounts for 80%, fossil fuels 16%, and renewables 3.4% (Community, 2016). Future energy demand in the EAC is also anticipated to triple by 2050 (Community, 2016). This data highlights that the majority of energy consumed in both East Africa and the broader continent is derived from biomass and fossil fuels. Kenya, like most African countries, has an ever-increasing population and fast-growing economies (Amos et al., 2020). This growth likewise comes with rising demand for energy, a precursor for economic progress and industrialization as seen earlier. High population growth is a characteristic of developing countries and, in most cases, is exponential (Maguta et al., 2021). This implies that energy demand will always grow in a logarithmic relationship to population.

A large percentage of energy used in Kenya comes from biomass (wood) at 62.5%, fossil fuels at 20.6% and renewable energy sources contributing 16.9% (Ibrahim et al., 2024). Fossil and wood

fuels take the largest share in the energy matrix (Dida et al., 2022). This means that the country heavily relies on conventional energy sources whose reserves, studies have shown, are steadily declining globally (Asaad et al., 2021). The decline may be attributed to the non-renewable nature of conventional energy sources and the environmental pollution associated with them (Devasani et al., 2021). These two factors triggered a match towards embracing renewable energy sources (Suphi & Cecilia, 2018) as from the year 1996.

In Kenya, renewable energy sources utilized include solar, wind, geothermal, biomass, and hydro. According to the Kenya energy statistics report (Mohammed et al., 2021), hydro and geothermal are the most widely used, each contributing around 29% to the electricity grid. In contrast, wind, and solar are less utilized, contributing 13% and 3% respectively, as shown in Table 1.

Table 1: Share of energy generation in Kenya as of the year 2022 (*Authority, 2021*)

	Installed MW	Effective MW	%contribution (Effective)
Hydro	838.1	809.1	28.9%
Geothermal	863.128	805.1	28.7%%
Thermal (MSD)	660.32	640.4	22.9%
Thermal (GT)	60	56	2.%
Wind	435.5	375.5	13.4%
Biomass	2	2	0.07%
Solar	90.25	90.3	3.2%
Interconnected System	2949.3	2788.4	99.5%
Off grid thermal	31.5	21.3	0.76%
Off grid wind	0.55	0	0.00%
Off grid solar	2.26	1.902	0.07%
Imports	0	0	0.00%
Total Capacity MW	2984	2802	100.00%

It is possible to use only renewable energy sources in Kenya if the concept of renewable energy mix is fully embraced. Renewable energy mix in this case means all the renewable energy sources are exploited. For this to happen, solar and wind energy exploitation must be prioritized since there

is huge power potential for both yet only a small percentage of that potential has been tapped. For instance, wind and solar energy potential was roughly estimated to be around 4600 MW and 15000 MW all over Kenya respectively (Chemengich & Masara, 2022). The estimated wind power potential alone is enough to suffice the country's energy needs, since the potential is twice as much as the country's energy demand.

1.1 Wind energy resource

Wind can be considered a mass of moving air mainly due to the density gradient of air molecules caused by pressure and temperature differences over the earth's surface. It is the kinetic energy of a moving mass of air. This energy is what is harnessed using wind turbines (John & Tony, 2015). The mechanical power produced by the turbines can then be converted to do useful work.

Studies show that Kenya has huge wind power potential based on the wind map developed by the Energy and petroleum regulatory authority (EPRA) (Authoriy, 2020), as shown in Figure 1. EPRA further indicates that 73% of Kenyan land experience favorable wind speeds of 6 m/s at 100 m height. In addition, 28228km² land experiences wind speeds ranging between 7.5 m/s to 8.5 m/s and about 2825km² experiences wind speeds between 8.5 m/s to 9.5 m/s (Authoriy, 2020). The data further confirms that there is indeed colossal wind power potential in Kenya, which remains untapped. Kenya has installed wind power capacity of about 436 MW, of which 25 MW is in Ngong Hills, 100 MW in Esilanke area in Kajiado county and 311 MW is on the eastern shores of Lake Turkana (Chemengich & Masara, 2022). The remaining locations in Kenya with favorable wind speeds are yet to be exploited.

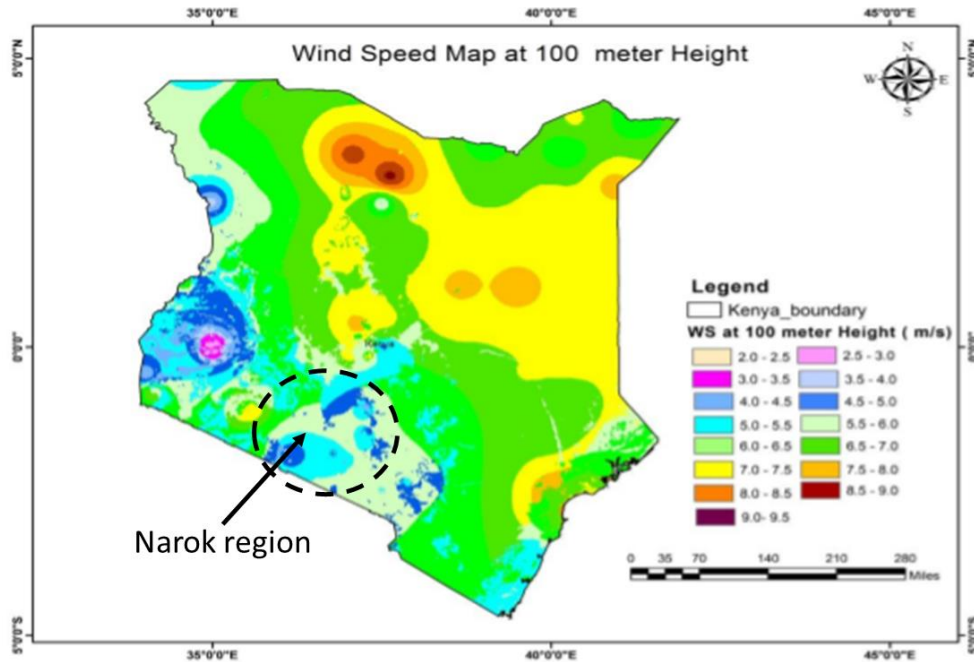


Figure 1:Kenya wind speed map as released by EPRA as of December 2019 (Authoriy, 2020).

The map clearly shows Narok County as one of the locations that have favorable wind speeds and, therefore, a potential site for wind energy extraction. Knowing that a place is lying within a windy region in a wind map is just but a first step in wind power viability assessment. The next crucial step is wind regime characterization and wind power density estimation which must be done prior to wind power extraction. Wind regime characteristics such as most probable wind speed, direction, distribution density, wind turbulence intensity, mean wind speed, wind speed spectra and wind power density are crucial information for exploiting wind energy. These characteristics are used in estimating wind power potential and designing wind farms. For instance, wind power density reveals whether a place is viable for commercial wind power extraction, that is, wind power density must exceed 200 W/m^2 to achieve economic viability. However, most of these wind characteristics in Narok County had either not been studied at all or only a few had been studied.

Therefore, this research evaluated these wind characteristics and approximated wind power density thereof for Narok County. The two parameter Weibull distribution and Morlet Wavelet decomposition technique were applied to the decadal (2011 to 2021) wind data of the county.

1.2 Weibull probability distribution function

Two parameter Weibull function is a probability distribution function (PDF) ideal for describing stochastic data sets such as wind speed regime of a given area. Indeed, the distribution has been reported by scholars to be the most reliable tool of analyzing most wind speed regimes of several areas around the world (Kalam et al., 2019). High accuracies of the PDF in wind speed data descriptions may be attributed to the simple, versatile and flexible nature of the PDF shown in equation 1.1. The PDF is versatile and flexible in the sense that its parameters are determined from the data that is being studied. Therefore, the PDF can fit wind regimes of various regions since the parameters are area specific. The scale parameter measures the location of the probability distribution curve along the wind speed axis. It is also known as a measure of mean wind speed and range. For instance, as scale parameter increases, the distribution curve shortens and becomes wider. Shortening and widening of the curve indicates that the range of observed wind speeds has widened and the number of higher wind speeds has also increased therefore increasing mean wind speed. The scale parameter has the dimensions of speed just like wind speed quantity. Shape parameter on the other hand is dimensionless and measures the probability of observing either low or high wind speeds of a regime. For instance, shape parameters ranging between 1 and 2 indicates that there is high probability of observing wind speeds $\leq 5.5 \text{ m/s}$ which are categorized as low wind speeds (Shu & Mike, 2021). The parameters are estimated through maximum likelihood approach as discussed in detail in chapter three. Equation 1.2 on other can be used to estimate wind power potential which is considered a better approximation of wind power density than traditional

direct calculation which only employs mean wind speed since equation 1.3 accounts for the probability of occurrence of chosen wind speed. Weibull cumulative distribution function ($F(x; c, k)$) in equation 1.3 gives the probability of wind speeds of an area not exceeding a chosen wind speed.. Moreover, plotting the actual cumulative distribution of wind speeds alongside the estimated cumulative distribution of wind speeds gives a good visualization of how well Weibull distribution describes the data. However, analytical evaluation of the Weibull's suitability in describing the wind regime can be done through error approximation techniques such as Root Mean Square Error (RMSE) and R-squared techniques (Abdoul et al., 2023).

$$f(x; c, k) = \begin{cases} \frac{k}{c} \left(\frac{x}{c}\right)^{k-1} e^{-\left(\frac{x}{c}\right)^k} & ; x \geq 0 \\ 0 & ; x < 0 \end{cases} \quad (1.1)$$

Equation 1 is a two-parameter traditional Weibull distribution where c & k are scale and shape parameters respectively whereas x can be any variable in this context, x is taken to be the observed wind speed (Mohamed et al., 2023).

$$P(v) = \frac{1}{2} \rho \int_0^{\infty} f(x; c, k) \bar{x}^3 dx \quad (1.2)$$

$f(x; c, k)$ is a probability distribution function (PDF), and v is the transient wind speed.

$$F(x; c, k) = \begin{cases} 1 - e^{-\left(\frac{x}{c}\right)^k} & ; x \geq 0 \\ 0 & ; x < 0 \end{cases} \quad (1.3)$$

1.3 Morlet wavelet decomposition

Wavelet decomposition is a mathematical technique that can be used to analyze the frequency content of a time series, such as wind speed data. By decomposing a time series into a set of wavelets, it is possible to identify and isolate different frequency components of the data, which

can provide insight into the underlying physical processes that are driving the variability of the wind.

In wind speed analysis, wavelet decomposition can be used to identify and analyze different frequency components of the wind speed data (Stefano et al., 2022), such as seasonal variations, and longer-term trends. The wavelet decomposition can reveal how the amplitude and frequency of these different components change over time, which can shed light into the physical processes causing the variability of the wind. For example, it can help identify the presence of diurnal wind patterns driven by daily heating and cooling cycles, seasonal variations influenced by changes in atmospheric conditions, or the impact of large-scale weather systems such as frontal passages or storm events on wind behavior.

One common approach to wavelet decomposition in wind speed analysis is to use the continuous wavelet transform (CWT) with Morlet as the mother wavelet, which decomposes the time series into a set of wavelets that are scaled and translated in time. The CWT can provide information on the amplitude and frequency of the different wavelets in the time series, which can reveal patterns and trends that are not visible in the raw data. Equation 1.4 and 1.5 are generalized CWT and Morlet wavelet respectively (Marta & Adam, 2022).

$$CWT_x^\psi(v; a, b) = \frac{1}{\sqrt{a}} \int_{-\infty}^{\infty} v(t) \cdot \psi\left(\frac{t-b}{a}\right) dt \quad (1.4)$$

$$\psi(t) = \frac{1}{\sqrt[4]{\pi}} \left[e^{i\omega_0 t} - e^{\frac{\omega_0^2}{2}} \right] e^{\frac{t^2}{2}} \quad (1.5)$$

Where, a , b , $\psi()$ denotes the scale, position parameter, and generalized mother wavelet, respectively. While, $v(t)$ is the signal being investigated. ω_0 is the central frequency of the mother wavelet.

The scale parameter in CWT represents the width of the analyzing wavelet in the frequency domain. In the context of wind speed analysis, smaller scales correspond to high-frequency variations in the wind speed, such as gusts, while larger scales correspond to low-frequency variations, such as changes in wind direction or speed due to weather patterns. While the location parameter can be thought of as a sliding window that moves along the time axis of the signal, allowing the analysis of the frequency content of the signal at different time instants. The location parameter indicates the time at which the wind speed is analyzed, and allows the detection of changes in wind speed over time (Eleonora et al., 2014).

1.5 STATEMENT OF THE PROBLEM

It has already been discussed in section 1.1e that the most reliable energy sources in Kenya are hydropower and geothermal. These sources provide the power base load demand of the country. However, hydropower is adversely affected by droughts, where during certain seasons, water volumes in rivers are reduced, consequently generating low electrical power. Utility providers resort to power rationing to cushion industries during peak demand. This is however not a permanent solution as it does not address the inevitable rise in future power demand arising from exponential population growth experienced by most African countries. The only way to solve the power problem is to diversify current power generation sources. One of the low-hanging fruits that can be exploited is wind energy, which remains largely unexploited in Kenya, especially in Narok County. However, this is currently not possible because relevant technical information on wind power potential, dominant wind direction, wind speed variability and spectral characteristics of the wind regime in Narok County is currently unavailable. Knowledge of these is critical for implementing a meaningful wind power project. This information gap could be responsible for the low exploitation of the wind power sector in Kenya. This research is an attempt to bridge this gap

by studying hourly wind data measured between 2011 and 2021. The research investigated mainly site-specific wind characteristics relevant to wind power generation, such as wind power density, wind speed variability with respect to time and height, most probable wind speed (or power), wind speed carrying maximum energy, dominant wind speed, wind turbulence intensity and wind power spectrum using mainly Weibull distribution and Morlet wavelet decomposition.

1.6 JUSTIFICATION

This research provides crucial technical information about the characteristics of the wind regime in Narok county. The availability of this information may encourage the installation of wind power plants in the region, which would help diversify the country's sources of power generation. This diversification is important because it reduces reliance on hydropower and other non-renewable energy sources, leading to a decrease in greenhouse gas emissions and a stronger response to climate change.

Moreover, the installation of wind farms in Narok county can enhance energy security and reduce dependence on imported fossil fuels, thereby benefiting both the county and the country as a whole. The identification of Narok as a suitable location for wind farms may attract investments in wind energy, fostering economic development in the area. This development can create job opportunities in manufacturing, construction, maintenance, and other related sectors.

Importantly, the research results eliminate the need to conduct a full wind power feasibility study in Narok, saving costs that would have been incurred by the government and other responsible bodies. Instead, the feasibility study can focus on other aspects such as assessing environmental impacts.

Additionally, the research findings have the potential to inspire innovation in wind power technologies specifically designed for the wind characteristics of the Narok region. This opens up new avenues for further research and contributes to the growth of knowledge within the scientific community. There are still recommended research areas that require additional investigation, creating opportunities for scholars to expand upon the existing body of knowledge.

1.7 GENERAL OBJECTIVE

To investigate wind characteristics and estimate wind power density of Narok weather station in Narok county using Weibull and Wavelet techniques.

1.8 SPECIFIC OBJECTIVES

- i. To determine the dominant wind direction in Narok County using wind polar chart analysis.
- ii. To fit the wind speed data using Weibull distribution
- iii. To characterize wind speed data using Morlet wavelet transform and Weibull distribution parameters
- iv. To determine the wind power potential of the site using the Weibull distribution

CHAPTER TWO

LITERATURE REVIEW

2.0 Introduction

In this section, a compilation of relevant studies conducted by scholars worldwide in the same field is presented. Section 2.1 focuses on reviewing similar or related researches conducted specifically on wind energy assessment around the country. In Section 2.2, a comprehensive examination is undertaken of the common techniques applied globally for the research objectives of this study.

2.1 Why the study area was chosen

Cheruiyot et al. (2016) characterized wind speed and estimated the wind power potential of the Kesses region in Kenya which exhibited unimodal and positively skewed characteristics. Implying that the wind speeds were dominated by low wind speeds (≤ 5.5 m/s). In the study, the two-parameter Weibull function was used to characterize the wind speed and estimation of wind power density using hourly wind data recorded for five years. The results indicated that the region had wind power densities of 41.24 W/m² and 228.91 W/m² at 10 m and 100 m heights, respectively. The average wind speed reported was 3.895 m/s and 6.926 m/s at 10 m and 100 m anemometer heights, respectively. The results suggested that the region is only suited for power generation at 100 m hub height. At 10 m, the power density falls into class 1 wind power density category since it is less than 100 W/m². Moreover, the results suggested that the wind speed increasing with increase in height as supported by the increased power densities at 100 m as opposed to 10 m.

A similar study, using the two parameters Weibull PDF, was done by Nyasani et al. (2018) at Kisumu city. The study established that wind energy in Kisumu city is only viable for domestic scale wind power extraction at 50 m turbine height. Mean wind speed that was recorded was 2.38

m/s at 10 m height. Annual wind power density at 50 m height reported was 127.99 W/m² which is classified as class II wind regime. Wind speed carrying maximum energy at 10 m height was reported to be 2.85 m/s. The same distribution was used to estimate wind power density in Eldoret and the results showed that the region has a mean wind power density of 80.379 W/m² at 20 m height with a mean wind speed of 2.5 m/s at 2 m height (Choge, 2015). Both Kisumu and Eldoret regions are not suitable for commercial wind power extraction since the reported wind power densities are 200 W/m².

Applying the same distribution as used in the previous paragraph, another study conducted in Marasabit and Garissa to determine the feasibility of wind power generation reported that the two counties are viable places for wind energy exploitation. The researchers similarly used Weibull PDF to characterize the wind speed and calculate the wind power densities of the two regions. Marsabit registered a higher wind power density of 2202 W/m² with a prevalent wind speed of 11 m/s, while Garissa registered a mean wind power density of 190 W/m² with a prevalent wind speed of 3.90 m/s. The results suggest that Marsabit is suited for grid-connected wind farms while Garissa County is not based on the 200 W/m² wind power density threshold requirement. However, Garissa would be suitable for commercial wind power extraction at higher heights than the 10 m since at higher heights, the wind speed increases. Marsabit county is also suitable for other domestic uses such as water pumping which requires higher wind speeds greater or equal to 10 m/s (Kamau et al., 2011).

Unlike the previously cited authors who used Weibull distribution alone, Ongaki et al. (2021) used Rayleigh distribution to estimate the wind power potential of Kisii region in Kenya. Apart from wind power potential estimation, the team also characterized the wind regime of Kisii County for different time-frames (daily, monthly, and annually). The results suggested that the region has a

wind power density of 29 W/m^2 and a mean wind speed of 2.9 m/s . Based on root mean square error analysis, Rayleigh PDF performed slightly better than Weibull for data in Kisii county. Similar research using the same analysis tools was conducted in Nyamira County but with hourly wind and direction data recorded for three months. Mean power densities reported for the area were 142.57 W/m^2 and 147 W/m^2 , obtained and estimated using Weibull and Rayleigh, respectively. The main motivation behind the choice of the two distributions was that the wind regime was unimodal. Using two distributions was for comparison and results validation purposes. In Nyamira, Weibull was reported to perform better than Rayleigh. Rayleigh was further away from the actual power density (135.30 W/m^2). The dominant wind direction was reported to NNW, and NW for the three months data used (Kwamboka et al., 2018).

Still on wind power density related studies, another study investigated wind resource potential for small-scale domestic wind turbines employing the combined empirical and computational fluid dynamics approach to investigate wind characteristics and compute wind power potential at Kenya's Kiseveni (in Machakos county) site. The results suggested that a small power density ranges between 31.65 W/m^2 and 54.00 W/m^2 at a height range from 40 m to 100 m . Based on the study, the area's wind regime was found to be class 1 wind, which means that the region is not suitable for grid-connected power generation systems but only for small-scale domestic wind power generation since wind power density is less than 100 W/m^2 (Justus et al., 19).

In Narok County, Kenya where the current study was conducted, there exists only one research related to wind power potential assessment. The reported research focused on investigating the best distribution that can model the wind speed distribution data of Narok County. The study compared the three parameter Gamma, three parameter Weibull and two parameter Weibull. The study utilized 2-year wind speed distribution data from Olderkesi. According to the study, the wind

regime studied was dominated by low wind speeds but not null wind speeds. Therefore, the three parameter Gamma fitted the data best because of low wind speeds and the third parameter (location parameter) defines the lowest occurring wind speed. The results vindicated three parameter Gamma distribution as the most preferred candidate (Otieno et al., 2021). The research, however, did not study the wind characteristics of Narok County.

In summary, some studies have been reported about wind energy assessment in some regions around the country, as sampled above. Among the studies that have been reported, there are still similar minimal studies that have been reported for Narok County, even though it is one of the regions marked as areas with favorable wind speed, as seen in Chapter One. The wind characteristics of Narok county remains vaguely understood and insufficient to inform design and development of wind power system. The research bridged this gap by characterizing wind speed, hence estimating wind power density for Narok County using decadal wind data from the Narok weather station.

2.2 Review of available wind data analysis tools

Wind analysis techniques must be employed to understand the wind regime characteristics of the study area which remain largely unknown as seen in section 2.1 of this chapter. So, it is reasonable to review the methods available, their strengths, and their weaknesses. Various researchers present different approaches in the literature that one can consider when analyzing wind data to gain knowledge of wind power potential and the wind speed frequency spectrum. Wind power potential is derived from stochastic wind data via PDFs, while wind speed frequency spectrum originates from signal analysis techniques. Several PDFs have been used to compute wind power density in different places around the globe. These PDFs used for wind power density estimation can be broadly classified as mixture PDFs and one-component (pure) distribution or persistence PDFs.

Mixture distribution models wind speed regime with more than one frequently occurring wind speed (multimodal) while one component distribution describes unimodal wind speed regime. Regarding spectrum analysis, a commonly used technique is the Wavelet Transform (WT) especially the Continuous Wavelet Transform (CWT) when it comes to wind data. These techniques will be discussed in this section.

2.2.0 Estimation of wind power potential using a mixture of PDFs

Mixture distribution is a combination of two or more distributions weighted according to their proportionate contribution to the mixture, and the summation of the weighting parameter must be unity (Ma, 2017). The distribution is normally applicable when computing the wind power density of multimodal data whose distribution can only be fitted by more than one distribution linearly combined. Weighting factor represents the proportion of the wind speeds distribution that a particular PDF in the mixture describes. Mixture distribution has been grouped in two, homogenous and heterogenous mixture as discussed in sections 2.2.1 and 2.2.2

2.2.1 Homogeneous mixture PDF used in WPD estimation

Homogenous mixture distribution has its components coming from the same type of distribution. For example, we have the Weibull-Weibull mixture (WW), Gaussian Mixture Model (GMM), Truncated Normal-Normal mixture (TNN), and so forth. This type of distribution describes multimodal wind speed regime where wind speed distribution profiles associated to each modal wind speed follow the same PDF species but the parameters for each component in the mixture are different. Parameters for each component of the mixture must be found independently. A few researchers worldwide have used this approach to estimate wind power potential, as evidenced by the papers sampled in the next paragraphs of which it is worth mentioning that homogenous models remain the most unexplored PDFs currently (Ma, 2017).

Gaussian mixture model (GMM) was used to estimate the wind power potential of multimodal wind speed data recorded for 54 years at Ijmuiden in Holland by Muhammad et al. (2020). In order to assess the suitability of the distribution in estimating wind power potential, its performance was compared to two-parameter Weibull (W2) distribution on the same data. The results showed the peak wind speed range was 6.43 m/s to 7.93 m/s, while wind power density was estimated to be 202 W/m². It was shown that GMM proved superior to standard two parameter Weibull according to Kurtosis and Skewness (K-S) test. It was also shown that GMM is suitable to model multimodal wind speed data with a confidence level of 95% as opposed to 2-parameter Weibull distribution (Ahmed et al., 2018). For short-term wind power density prediction, Weibull proved to be superior to GMM implying that, wind speeds within short period of time were unimodal and positively skewed. The accuracy of GMM relies heavily on the correct approximation of the parameters for the component distributions and the number of components based on the regime of the wind being studied. The wind speed characteristics were shown to depend on the height at which the wind speed data was collected. This means, the greatest challenge of this approach is correctly estimating parameters considering the wind speed regime and deciding on how many components should be present in GMM.

Apart from GMM mixture model that has been applied in wind speed analysis, 2-component Weibull-Weibull (WW) mixture model can also be applied to study multimodal wind regime as demonstrated by Jaramilo et al. (2004). WW mixture was used to study wind speed characteristics relevant to wind power density approximation in Mexico at a station called La Ventosa (Jaramilo & Borja, 2004). The authors chose the distribution because the wind regime displayed bimodal characteristics. Weibull-Weibull mixture was reported to be better in estimating the Capacity Factor (CF) of wind turbines installed in the area. CF registered using WW was 0.58, while that

of two parameter Weibull distribution was 0.51. The researchers also showed that two parameter Weibull underestimated the probability of occurrence of wind speed between 12 to 20 m/s and overestimated wind speed occurring between 4 and 12 m/s. Based on the reported results, WW was concluded to be better in bimodal wind data analysis compared to Weibull distribution. Reported challenges associated with this approach were generally similar to the ones mentioned in the last paragraph.

2.2.2 Heterogenous mixture distribution used in WPD estimation

Heterogeneous mixture distributions describe multimodal wind regimes where wind speed distribution profile associated to each modal wind speed is described by a unique species of PDFs. Similarly, each component of the mixture has different parameters. These distributions are similarly applied to assess wind power potential for multimodal wind regimes. Examples of such distributions include; Gaussian Weibull mixture, Lognormal Weibull (LW), etc. This type of distribution is the most widely used in this category as opposed to the homogenous case. Some cases of heterogenous mixture distributions are described below.

Gugliani et al. (2017) studied wind power density employing a number of mixture models such as Weibull-Weibull, Gamma Weibull mixture (GW), Truncated Normal Weibull (TNW), Truncated Normal-Normal (TNN), Truncated Normal Gamma (TNG), Gamma-Gamma (GG) and Maximum Entropy Principle (MEP) based distributions. They compared the performance of the mixture models with the conventional two parameter Weibull (W2) for three different sites in India, namely, Calcutta, Ahmedabad, and Trivandrum stations. The mixture models showed superiority over two parameter Weibull and MEP distributions in all three sites suggesting that the wind regimes in all of them were multimodal. Truncated Normal Weibull mixture performed the best and managed to estimate the wind energy to an accuracy of 99.80% according to RMSE and R^2

test in Calcutta station. Error in approximating wind power density of the station was reduced to 5.12 % when TNW distribution was used from the 10.49% error previously registered when two parameter Weibull distribution was used. Truncated Normal Gamma distribution best fits the wind power density histogram in the Ahmedabad station. The error was reduced from 6.78% registered by two parameter Weibull to 3.91% when Truncated Normal Gamma was used. Lastly, Truncated Normal Gamma also outperformed other distributions in the Trivandrum site. The results also showed that MEP distributions registered the least performance; therefore, it's unsuitable distribution in estimating wind power potential for the studied sites. The authors clearly articulated that none of the mixture distributions investigated could model wind regimes dominated by low but non-stationary wind speeds. According to the research, the most qualified distributions (TNW and TNG) are given by equations 2.1 and 2.2.

$$\varphi(x; \lambda, k, \mu, \sigma, a) = af(x; \lambda, k) + (1 - a)q(x; \mu, \sigma) \quad (2.1)$$

Where; $q(x; \mu, \sigma)$, μ , and σ represents the truncated normal distribution, mean and standard deviation, respectively. Other terms bear the same meaning as earlier defined. The truncated normal distribution is given in equation 2.3.

$$q(x; \mu, \sigma) = \int_0^x \frac{1}{I(\mu, \sigma)\sigma\sqrt{2\pi}} \exp\left[-\frac{(x-\mu)^2}{2\sigma^2}\right] \quad (2.3)$$

Where; $I(\mu, \sigma)$ is the normalization factor.

$$\varphi(x; \lambda, k, a, b, w) = wq(x; \mu, \sigma) + (1 - w)f(x; a, b) \quad (2.4)$$

Where; equation 2.4 is the TNG distribution, w is the weighting factor for this model and $f(x; a, b)$ is the Gamma distribution.

Weibull-Weibull, Gamma Weibull (GW), and Lognormal Weibull (LW) mixtures were similarly used to estimate the wind energy output of the actual wind turbine installed in Narakkhalliya, Sri Lanka, by (Rajapaksha & Kanthi, 2016) using wind speed recorded in the area. It was found that Weibull-Weibull mixture distribution registered the least error margin in approximating the energy of the place as compared to the actual energy produced by the actual turbine located in the area. The energy output of the turbine was measured at 40 m turbine height. The distribution registered an accuracy level of 83.2%, while 2-parameter Weibull registered an accuracy of 75%. The research also reported that Weibull-Weibull accuracy in energy approximation drops slightly when wind speeds exceed 11 m/s. The main challenge presented by the authors is the computational cost required when estimating the parameters of the distributions. Equations 2.5 and 2.6 present LW and GW, respectively.

$$\varphi(x; \lambda, k, \mu, \sigma, a) = af(x; \lambda, k) + (1 - a)\ln[q(x; \mu, \sigma)] \quad (2.5)$$

Where $\ln[q(x; \mu, \sigma)]$ is the lognormal distribution which is the natural log of the normal distribution.

$$\varphi(x; \lambda, k, a, b, w) = wf(x; \lambda, k) + (1 - w)f(x; a, b) \quad (2.6)$$

2.2.3 Estimation of wind power potential using One component (persistence) PDFs

This category of distributions best models wind power density for areas with unimodal wind speed regimes. Most of these distributions are parametric in nature (Hanbo et al., 2022). PDFs in this category are usually simpler as compared to mixture distribution in almost every aspect. Some of these PDFs are reviewed below.

Rayleigh distribution was used to assess wind power density in Romania of a rightly-skewed unimodal wind speed regime. Such wind speed regime is dominated by low to medium wind speeds which mostly lie in the range 2 m/s to 6 m/s. Wind power density calculated using the distribution was recorded to be 295.4 W/m², which was an error margin of the real power density estimation by about 4.03% (Lizica et al., 2019). The margin of error associated with Rayleigh distribution was shown to increase when wind speed regime is dominated with low wind speeds. In another study which compared the performance of five different distributions (Normal, Rayleigh, Weibull, Chi-Square and Gamma) in estimation of wind power density of Pakistan coastline, showed that Rayleigh had the worst performance. The results presented a case where unimodal wind regime has a normally distributed wind speeds where the mean, median and modal wind speed are closer to each other like in the case of Pakistan coastline. Because of this wind regime, Normal distribution ranked as the best distribution followed by the Weibull distribution. Reported estimated wind power density based on Normal distribution was ranging between 147.44 W/m² to 187.87 W/m² in all the sites that were investigated (Muhammad et al., 2021). However, most wind regimes are not normally distributed, rendering the applicability of the normal distribution restricted to only specific areas that have normally distributed wind regimes (Pritha, 2020; Nawel et al., 2018).

Unlike the wind regime of Pakistani coastline, most wind regimes are either negatively or positively skewed; where positively skewed wind speed data indicates that occurrences of low to medium wind speeds are more frequent, while strong or high wind speeds occur less often but with greater intensity when they do occur while for negatively skewed, the opposite is true. Approximation of wind power density of such wind regimes have been predicted by two parameter Weibull distribution (Ivana et al., 2017). For instance, two parameter Weibull distribution was

deployed in Mwingi to estimate wind power densities occurring at varying heights (60 m, 80 m, and 100 m). The wind power densities that were reported were; 84.3 W/m², 100.5 W/m², and 115 W/m² respectively. The wind energy potential of Machakos County in Kenya was investigated using the same distribution by Kennedy et al. (2023). The researchers reported a wind power density of 17 W/m² (Kennedy et al., 2023). A similar study was conducted in Galati County in Romania where Weibull and Rayleigh were used to estimate wind power density. Two distributions were used for results comparison and validation. Rayleigh distribution overestimated wind speeds ranging between 1-3 m/s by about 4.71% while it underestimated wind speeds ranging between 4-9 m/s by 2.46%. Weibull on the other hand recorded underestimation of 0.24% and overestimation of 0.02% in the respective ranges. Based on Weibull distribution, wind power density recorded for the area was 361.97 W/m² which was a slight overestimation of the power by 10.21 W/m² (Kiche et al., 2019)

In general, most scholars have hailed either two parameter Weibull or its variance as one of the most applied distributions in wind energy analysis, especially for estimating Wind Power Density (WPD) (Younes et al., 2019). That is, Weibull PDF accurately describes most wind regimes for different places around the world compared to any other distribution even among the established distributions. This might be attributed to the simplicity, flexibility, and versatile nature of Weibull and the fact that a lot of established information is available about the distribution. Additionally, in studies involving new models or modified models, Weibull distribution has been used as a standard (Kengne et al., 2020). Considering all these factors and weighing all distributions on a balance against the scope of this work, Weibull distribution is the most desirable distribution. Based on the literature reviewed so far, it is clear that two parameter Weibull has never been employed to characterized wind regime in Narok especially data from Narok weather station.

Therefore, the distribution was employed to characterize wind regime in Narok using data from Narok weather station.

2.3 Parameter estimation methods

Most of the distributions that are used to analyze wind in literature are parametric in nature, although there exist non-parametric methods, such as spline-based, kernel-based methods, etc., that are well documented in (Munir et al., 2017). However, the non-parametric methods are usually complex to implement yet their accuracy is low comparable to the parametric methods. This work focused on two parameter Weibull PDF, which is a parametric distribution. Parameter estimation methods that are commonly employed to estimate Weibull parameters are discussed below

Nil et al. (2020) investigated different methods used for Weibull parameters to establish the most effective method. The methods that were studied are inclusive of Maximum Likelihood Estimate (MLE), Method of Moment (MOM), Least Square Method (LSM), Method of Logarithmic Moment (MLM), Percentile Method (PM), and L-Moment method (LM). These methods were then compared to Mean Square Error (MSE) and Mean Absolute Percentage Error (MAPE) methods. The results indicated that for large sample data sizes, MLE is the best in estimating parameters for two parameter Weibull PDF, followed closely by LM. Among the numerical methods, the MLE method estimates the parameters more efficiently than its counterparts listed previously. It is the primarily used technique to estimate Weibull parameters. Therefore, the MLE technique was employed in this research to estimate the parameters.

2.4 Performance indicators

Performance indicators are methods used to assess the suitability of a given wind distribution estimation method used in the analysis of WSD and therefore considered as error estimation methods. With the aid of these methods, one can know how well the fitted distribution describes

the actual data distribution. RMSE and coefficient of determination (R^2) were employed by (Cherinet et al., 2020) to assess the suitability of parameters obtained via MOM, Empirical Method (EM), and Graphical Method (GM). Parameters were obtained from Rayleigh and W2 distributions. The analysis also revealed that the multiple criteria approach in analyzing wind data is plausible and gives better insights of the actual wind regime. It was also noted that RMSE gives better insight into judging the statistical methods used, while (R^2) gives better insight into power production. In this research, RMSE and R^2 was used as accuracy judgement criteria.

2.5 Continuous Wavelet Transform (CWT) as applied to wind data

Decomposition of signals using CWT technique requires a basis wavelet upon which other waves can be generated via transformation called mother wavelet. There are several mother wavelets that one can choose from; the choice depends on the signal to be processed. Some of the mother wavelets applicable to wind decomposition are presented below.

Antonio et al. (2019) used Morlet wavelet decomposition technique to detect missing data from time series wind data measured for a period of 11 years in 10 min interval. The researchers then explored various techniques such as moving average to fill the identified missing data. To evaluate the best data filling technique, Morlte wavelet decomposition analysis was employed. The scalograms generated from the decomposition of wind data have the ability to unveil the underlying seasonal cycles present in the data. Consequently, any anomalies within these cycles can be readily identified through pattern breaches that maybe observed in the scalogram plot. When Morlet wavelet is used to extract seasonal features of data, the central frequency is normally set between 5-6 Hz. At this range, a good balance between frequency and time resolution can be achieved (Antonio et al., 2019).

The same signal decomposition technique was employed by (Tian et al., 2017) to study oscillation characteristics of wind speed, temperature and solar radiation. The researchers used Morlet wavelet decomposition to identify the periodic behavior of the aforementioned weather elements. The researchers demonstrated that the technique is capable of detecting seasonal patterns from the three data sets and identify the correlation pattern among the three elements by comparing the scalograms plotted for each element coupled with cross wavelet transformation technique. Morlet wavelet have also been reported to be applicable in extraction of inherent seasonal or periodic properties of signal in other related fields such as study of wind induced ocean waves, geophysical time series signals, thunder-storm induced mean wind velocities etc (Elsayed et al., 2004). In general, when periodic or seasonal inherent properties of a signal are needed, then Morlet wavelet decomposition is the best technique to employ with central frequency in the range of 5-6 Hz.

CHAPTER THREE

METHODS

3.0 Introduction

In this chapter, methods that were employed during the research process have been discussed. The techniques include; Polar chart analysis, two parameter Weibull PDF analysis, Maximum likelihood estimate, R^2 & RMSE, statistical mean, wind speed extrapolation law and Morlet wavelet transformation. The methods were used for; wind direction analysis, wind speed characterization and wind power density estimation, parameter estimation, error analysis, mean wind speed calculation, wind speed extrapolation and wind speed spectrum analysis respectively.

All the methods were executed in MATLAB program version R2018a.

3.1 Data Acquisition and Filtering

Decadal (2011 to 2021) Wind Speed Data (WSD) measured at 10 m height and Wind Direction Data (WD) for the Narok weather station in Narok county was obtained from Kenya Meteorological Department station headquarters in Nairobi, Kenya. Narok county is located in Rift Valley region as indicated in figure 1, the county borders Tanzania to the south, Nakuru to the North and Kajiado county to the East. Narok weather station on the other hand is bound by the geographical coordinates 1.0918° S, 35.8498° E.

The data was inspected for invalid entries such as non-number entries, empty cells, negative entries, and entries more than 25 m/s (exaggerated entries). Wind speeds exceeding 25 m/s are

considered invalid since most wind turbines are designed to cut-out at this wind speed to avoid turbine damage due to stormy winds. All the anomalies that were found in the data were counted and their proportion with respect to the entire data set calculated. The percentage was about 0.0033% which is way below the allowable maximum percentage of 3%. The threshold missing data is set at less than 3% to ensure the accuracy of the obtained result. If a large number of data points are missing, then the accuracy of the results is compromised. For instance, wind power density is proportional to the cube of wind speed. If a slight error is introduced by a large number of missing data points, this error will be cubed in the final results.

To remove the anomalies, the data was then subjected to digital filtering on the MATLAB platform following the procedures given below.

- i. The multidimensional matrices of the wind speed and wind direction data were converted to n by 1 matrix and the matrices were assigned to A and WD respectively. Where A is a matrix containing wind speed, while WD is a wind direction matrix. A and WD have the same dimensions and number of elements since wind speed and wind direction are measured simultaneously.
- ii. Each data entry in A or WD corresponds to a specific date and time the data entry was recorded. Therefore, A and WD could further be subdivided into corresponding data sets of hour, month and year designated as pointer matrices B, C, and D respectively. Figure 2 shows a snapshot of how these pointer matrices were constructed whereby in the first column we have the date that the wind speed and wind direction were recorded; the second column gives the time; the third column shows the month; the fourth column shows the year. Matrix A is for wind speed, matrix B is for time, matrix C is for the month, matrix D is for the year and matrix WD is for Wind Direction.

Date	hours	month	year	wind speed	wind direction
12/31/2012 17:00	17	12	2012	3.8	140
12/31/2012 18:00	18	12	2012	3.6	90
12/31/2012 19:00	19	12	2012	3.6	120
12/31/2012 20:00	20	12	2012	3.3	100
12/31/2012 21:00	21	12	2012	3.5	0
12/31/2012 22:00	22	12	2012	3.2	0
12/31/2012 23:00	23	12	2012	3.3	350
1/1/2013 0:00	24	1	2013	3	320
1/1/2013 1:00	1	1	2013	3.2	340
1/1/2013 2:00	2	1	2013	3.5	350
1/1/2013 3:00	3	1	2013	3.6	340

Figure 2: Snapshot illustrating how matrices A, WD, B, C and D were made.

- iii. The wind speed matrix A was checked for invalid entries (NaNs, negatives, empty entries and entries exceeding 25 m/s), all the invalid entries were counted and the percentage contribution of the invalid cells were calculated. The percentage was less than the 3 % therefore the filtration proceeded to the next step.
- iv. Where invalid entries occurred consecutively more than six times in a row in A, indices corresponding to the consecutively occurring invalid entries were identified. The entries corresponding to the identified indices in matrices A, WD, B, C and D were deleted to preserve the dimensions of the matrices and the corresponding times. Deleting all the entries that occurred more than six consecutive times preserves the accuracy of the data. For example, a day having more than six invalid entries translates to more than 25% of data recorded on that day being invalid. Which when not taken care of will eventually affect the overall accuracy of the data.

- v. The remaining invalid entries in A were then substituted through moving average technique. The entries that exceeded 25 m/s were set to 0 m/s. Even though there were virtually no wind speeds observed that exceeded 25 m/s. Wind turbines don't generate any power beyond the cutout wind speed. Most wind turbines have their cutout wind speed at 25 m/s. Therefore, it is reasonable to set all wind speeds >25 m/s to zero since power generated at such speeds is zero.
- vi. The steps above leave matrix A completely filtered while WD may still have some anomalies. To take care of the remaining anomalies in WD, the manipulated matrices A, WD, B, C and D are then subjected again to steps iii-v with WD as the reference matrix instead of A. That is, WD and A will exchange roles (positions) so that the anomalies will now be NaNs, negatives, empty entries and entries exceeding 360°. Since direction data cannot exceed 360°, any entry exceeding this value must be treated as an anomaly. All the entries that exceeded 360° were set to 360° even though there were virtually no such entries in the data. All other invalid entries were similarly filled using moving mean technique.

Step i-vi above were executed in MATLAB through scripting, the general logic that were used to develop the scripts for data filtration have been displayed in the appendix.

3.2 Wind direction determination

The dominant wind direction was determined from filtered data obtained in 3.1 above. Filtered wind speed data and wind direction data were used to prepare frequency distribution table as illustrated in Table 2. Wind direction data was subdivided in an interval of ten to capture the possible wind directions from the wind data as much as possible. This is because the instrument that was used to take wind direction measurements rounded off the wind direction data to the nearest tens according to the nature of data that was provided. All the data entries were recorded to the nearest tens. Wind speed was then grouped in intervals of 5 m/s just for convenience so that the polar chart wouldn't be crowded. The frequency distribution table was used to plot the polar charts. Equation 3.1 was used to convert frequencies of each group into percentages. Similarly, all the calculations and polar charting were done in MATLAB environment. The corresponding flowchart that guided scripting for this analysis has been displayed in the appendix.

Table 2: Illustration of how the frequency distribution of the wind direction verses wind speed was done

Direction category	Number of observations per category		
	0-5 (m/s)	5-10 (m/s)	10-15 (m/s)...
0-10	f ₁	f ₂	f ₃
11-20	f ₄	f ₅	f ₆
21-30	f ₇	f ₈	f ₉
⋮	⋮	⋮	⋮

$$\%frequency = \frac{f_i}{\sum_i^n f_i} \times 100\% \quad (3.1)$$

3.3 Mean wind speed and standard deviation

Mean wind speeds for Narok County that were established include; hourly, monthly, and annual mean wind speed. Hourly mean wind speed was found by averaging all the wind speed observations that occurred for each hour of the day over the entire period the data was collected to come up with a single value for each hour of the day. This analysis resulted into 24 values which were then plotted to come up with diurnal mean wind speed variation chart. Monthly mean wind speed was found for each month of the year by averaging all the observations that occurred in each month of the year. Total of twelve values were yielded that corresponded to all the months of the year, these values were then plotted on a bar graph to depict monthly mean wind speed variation of the year. Annual mean wind speed was taken to be the average of all the observations recorded over the entire period, this yielded a single value. The formula for calculating the mean wind speed has been generalized as in equation 3.2.

$$\bar{v} = \frac{1}{n} \sum_i^n v_i \quad (3.2)$$

\bar{v} is the mean wind speed; v_i wind speed, and n is the number of observations within the period.

The standard deviation in diurnal and monthly mean wind speeds on the other hand was calculated using equation 3.3.

$$\sigma = \sqrt{\frac{\sum_i^n (v_i - \bar{v})^2}{n}} \quad (3.3)$$

σ is the standard deviation, \bar{v} is the mean wind speed, v_i is the wind speed, and n is the number of hours/months/days within the considered period.

Equations 3.2 and 3.3 were both implemented in MATLAB environment and the corresponding flowcharts that guided the implementation are found in the appendices.

3.4 Wind speed variability with a hub height

Annual mean wind speed obtained above was used to calculate wind speed variation according to hub height varied from 10 m to 100 m by extrapolation. 100 m is the maximum height beyond which no meaningful energy can be extracted from the wind. Equation 3.4 was executed to accomplish this purpose. A graph of the extrapolated wind speed against hub height was plotted. All calculations and plotting were done in MATLAB environment.

$$v_z = v_s \left(\frac{z}{10} \right)^b \quad (3.4)$$

Where v_z is the extrapolated mean wind speed at a given height, v_s represents mean wind speed at 10 m height, z is the height, and $b = 0.3$. The constant b is called wind shear constant and is chosen based on the ground characteristics of the area. For areas characterized by small towns, suburbs with buildings that are low to medium rising, b is assumed to be 0.3 while cities with high rising buildings b is assumed to be 0.4 (Ali et al., 2020; Francisco et al., 2019). Definition of high-rising building varies in different regions and contexts; however, commonly adopted method of definitions is using the number of floors and the actual height of the building. For example, in United States, National Fire Protection Association (NFPA) definition code of 2012 categorize any building that is taller than 75 feet as high-rising. 75 ft building translates to about 5-7 floors. National Building Code (NBC) of India on the other hand categorize any building having more

than four floors which is about 50 ft as high-rising. Narok weather station is located arguably within Narok town. Narok town is characterized by shrubs, trees and buildings that are mostly below 50 ft tall. Only few buildings have five floors and there's virtually no building that exceed this height. Therefore, it's reasonable to choose b for Narok as 0.3.

3.6 Turbulence intensity variation

Daily (diurnal), monthly, and annual mean wind turbulence intensities were calculated using equation 3.5. A graph of wind turbulence intensity against time were plotted for each case. Similarly, all calculations were executed in MATLAB software.

$$I = \frac{1}{N} \left(\sum_i^N \frac{\sqrt{(\sigma_i)^2}}{\bar{v}} \right) \quad (3.5)$$

Where σ & \bar{v} represents standard deviation and mean wind speed, respectively, other terms bear their normal meanings.

3.7 Weibull parameters

Weibull parameters were obtained using MLE. The inbuilt subroutine (`wblfit()`) in MATLAB program were used to estimate these parameters. In MLE, the log-likelihood function (which is obtained from the likelihood function in equation 3.6) is first obtained, as indicated in equation 3.7. The function is then partially differentiated with respect to shape and scale parameters which are then equated to zero to obtain the shape and scale parameters.

Likelihood function is obtained by equation 3.6, it represents the maximum probability of all the observed wind speeds.

$$L(x; \lambda, k) = \prod_{i=1}^N \frac{k}{\lambda} \left(\frac{x_i}{\lambda} \right)^{k-1} e^{-\left(\frac{x_i}{\lambda} \right)^k} \quad (3.6)$$

$$\ln(L(x; \lambda, k)) = \ln \left[\prod_{i=1}^N \frac{k}{\lambda} \left(\frac{x_i}{\lambda} \right)^{k-1} e^{-\left(\frac{x_i}{\lambda} \right)^k} \right]. \quad (3.7)$$

$$\therefore \ln(L(x; \lambda, k)) = N \ln k - N k \ln \lambda - \sum_{i=1}^N \left(\frac{x_i}{\lambda} \right)^k + (k-1) \sum_{i=1}^N \ln x_i \quad (3.8)$$

Equation 3.7 is then partially differentiated with respect the parameters λ and k as follows;

$$\frac{\partial L(x; \lambda, k)}{\partial \lambda} = \delta = \frac{-Nk}{\lambda} + k \sum_{i=1}^N x_i \frac{1}{\lambda^{k+1}} = 0. \quad (3.9)$$

$$\frac{\partial L(x; \lambda, k)}{\partial k} = \sigma = \frac{N}{k} - N \ln \lambda - \sum_{i=1}^N \ln \left(\frac{x_i}{\lambda} \right) e^{\ln \frac{x_i}{\lambda}} + \sum_{i=1}^N \ln x_i = 0 \quad (3.10)$$

From equations 3.9 and 3.10, are then partially differentiated again with respect to λ and k to form elements of Jacobian matrix as shown in equation 3.12;

$$J = \begin{bmatrix} \frac{\partial \delta}{\partial \lambda} & \frac{\partial \delta}{\partial k} \\ \frac{\partial \sigma}{\partial \lambda} & \frac{\partial \sigma}{\partial k} \end{bmatrix} \quad (3.11)$$

The Jacobian matrix formed in 3.11 above can easily be shown to be non-singular and symmetric as detailed in (Shaima & Iden, 2021), therefore, equation 3.12 follows.

$$\begin{bmatrix} \lambda_{i+1} \\ k_{i+1} \end{bmatrix} = \begin{bmatrix} \lambda_i \\ k_i \end{bmatrix} - J^{-1} \begin{bmatrix} \delta(\lambda_i) \\ \sigma(k_i) \end{bmatrix} \quad (3.12)$$

Hence;

$$\lambda = \left(\frac{1}{N} \sum_{i=1}^N x_i^k \right)^{\frac{1}{k}} \quad (3.13)$$

$$k = \left[\frac{\sum_{i=1}^N x_i^k \ln x_i - \overline{\ln x}}{h \sum_{i=1}^N x_i^k} \right] \quad (3.14)$$

Once equation 3.14 is solved via iteration methods, the solution obtained is substituted back to equation 3.13 to obtain the second parameter. The above was implemented in MATLAB, refer to appendix to see the flowchart associated to the implementation.

3.8 Measured and estimated Weibull densities

The next task was to estimate Weibull probability densities by substituting the obtained parameters and observed wind speeds into the Weibull PDF in equation 1. Then, actual probability densities were calculated by grouping the filtered mean wind speed data into a frequency distribution table similar to that in Table 2. The interval of each wind speed group was set at 0.5 m/s. This interval size was chosen for convenience, as it would result in 50 bins (groups), which provided a better visualization of the data. Then frequency of each category was substituted into equation 3.15 to calculate the actual probabilities. The estimated and actual probability densities were then plotted on the same axes with wind speed being on the x axis while probability densities on the y axis. Similarly, all the calculations were carried out in MATLAB environment. Refer to appendix to view the flowchart that guided the implementation.

$$\text{Actual probability density} = \frac{\text{Number of observation in each category (frequency)}}{\text{total number of observation}} \quad (3.15)$$

3.9 Wind speed carrying maximum energy and most probable wind speeds

The most probable wind speed and wind speed carrying maximum energy were obtained using equations 3.16 and 3.17. Equation 3.18 was used to calculate maximum wind power of the selected site (Mekalathur et al., 2019).

$$v_{mp} = c \left(\frac{k-1}{k} \right)^{1/k} \quad (3.16)$$

$$v_{maxE} = c \left(\frac{k+2}{k} \right)^{1/k} \quad (3.17)$$

Where; v_{mp} , v_{maxE} , k and c represents most probable wind speed, wind speed carrying maximum energy, shape and scale parameters.

3.10 Wind power densities

Monthly and overall mean wind power densities were calculated using equation 3.18 in MATLAB environment. Wind power variation at different heights was assessed through extrapolation using equation 3.18 but with extrapolated values of c and k calculated using equations 3.19 and 3.20 respectively. Most probable wind power density of the other hand was calculated using equations 3.21 (Daoudi et al., 2019).

$$\bar{P} = \frac{1}{2} \rho c^3 \Gamma\left(\frac{k+3}{k}\right) \quad (3.18)$$

$$c_z = c \left(\frac{z}{10m}\right)^b \quad (3.19)$$

$$k_z = \frac{k}{1-0.088 \ln(z/10)} \quad (3.20)$$

$$P = \frac{1}{2} \rho \overline{v_{mp}}^3 \quad (3.21)$$

All terms in equations 3.18-3.21 have their normal meanings as earlier defined.

3.11 Wind speed spectral analysis using CWT

CWT, defined in equation 1.4 with Morlet as the mother wavelet defined in equation 1.5, was used to mine the spectral behavior of the wind regime of Narok County. The scale range was defined to be between 1 to 256. This range provided a good trade-off between the frequency resolution and localization of the frequencies in time. Moreover, the scale is capable of capturing both low and high frequencies in a wind regime. For example, lower scales correspond to higher frequencies as

dictated by equation 3.22. Each scale chosen corresponds to a specific wavelet frequency as implied by equation 3.22, the contribution of that wavelet in the signal is computed by combination of equation 1.4 and 1.5. The output of equation 1.4 is just coefficient which quantifies how much a wavelet (wind speed of given frequency cycle) of a specific frequency is present in the wind regime over time. Since the data was an hourly data, the time interval was adopted to be 1. After decomposition, the frequencies were plotted against time and the power of each frequency in the signal was denoted by the color in the chart. Bright yellow being the highest power and dark blue being the lowest power. Similarly, signal decomposition using CWT was performed in MATLAB environment.

$$f(t) = \frac{1}{\log(a)dt} \quad (3.22)$$

Where, $a = 1$ to 256 & $dt = 1$

3.12 Error approximations (PDF performance analysis)

The performance of two parameter Weibull PDF was judged by two methods, namely; RMSE defined by equation 3.23 and R^2 defined by equation 3.24.

$$RMSE = \sqrt{\frac{\sum_i^N |y_i - \hat{y}_i|^2}{N}} \quad (3.16)$$

$$R^2 = 1 - \left(\frac{\sum_i^N |y_i - \hat{y}_i|^2}{\sum_i^N |y_i - \bar{y}|^2} \right) \quad (3.17)$$

Where $y_i, \hat{y}_i, and \bar{y}$ represent actual, predicted and average value respectively. N stands for number of observations.

CHAPTER FOUR

RESULTS AND DISCUSSIONS

4.0 Introduction

In this chapter, the results that were obtained from the analysis are presented alongside their interpretations and discussions

4.1 Wind direction

Figure 3 shows wind direction at different wind speeds for Narok weather station and its environs. The predominant wind direction was found to be East (E). From the figure, about 25% of the time-

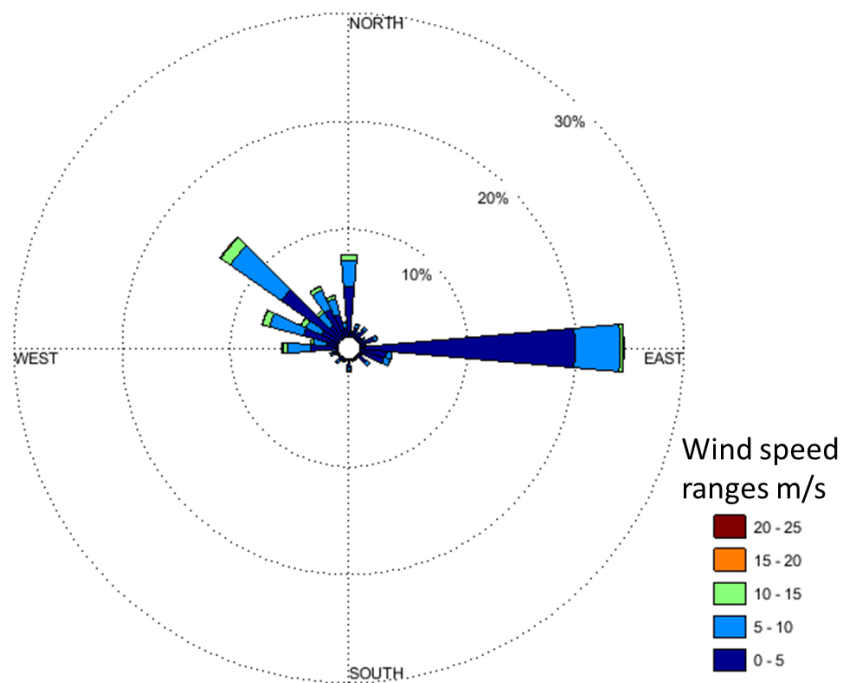


Figure 3: Polar chart demonstrating wind directions over different wind speed ranges for Narok weather station.

wind was blowing from the east direction. These observations are consistent with the ones made by Weather spark Kenya. The published information in the organization's website confirms that wind predominantly blows from the east (weatherspark.com, n.d.). This observation might be attributed to the fact that Narok is bordered to the east side by colder regions such as Limuru in Kiambu county and to the west by warmer regions such as Migori county. Moreover, Narok typically experiences higher temperatures compared to the regions neighboring it to the east as aforementioned. This temperature difference leads to air density gradient since the air molecules to the eastern side would be typically denser due to colder temperatures as compared to the western side which is characterized by warm temperatures. The density gradient will therefore trigger mass flow of air molecules from the east towards the west, which explains why the predominant wind direction is east. From the same figure, it is evident that some of the winds were originating from generally North West side. These winds are mainly originating from Mau Forest which is equally colder compared to other regions of Narok especially around the vicinity of Narok town where Narok weather station is situated. Wind blowing from the east is dominated by wind speeds ranging between 0 m/s to 5 m/s. This implies that domestic scale wind turbines that have cut-in and rated wind speeds to be $\leq 5 \text{ m/s}$ with power rating $<100 \text{ kW}$ should be oriented facing the east direction to operate optimally. For grid-tie installation wind turbines which have their cut-in wind speeds more than 5 m/s and rated power $>100\text{kW}$ should be installed facing NW direction with the ability to yaw about an angle of at least 90° according to change in the wind direction. This is because most wind speeds ranging between 5-15 m/s are predominantly from the directions bound by North and West directions quadrant as evident in Figure 3. In general, wind speed directions of Narok county ranges from East to West in an anticlockwise direction as most (about 80%) of the polar chart arms lie within the area. Therefore, wind turbines with the ability to yaw about 180° is the

most suitable turbines for wind farms in the area, approximately 80% of all the wind speed ranges will be captured as indicated in Figure 3. In Narok weather station and its vicinity, directionally static wind turbines are not recommended since they would only extract wind power blowing from the direction along which the turbine is oriented, therefore extracting only a portion of the available wind power.

4.2 Mean wind speeds and standard deviation

4.2.1 Hourly mean wind speed

Figure 4 displays mean wind speed evolution with respect to the hour of the day at 10 m height.

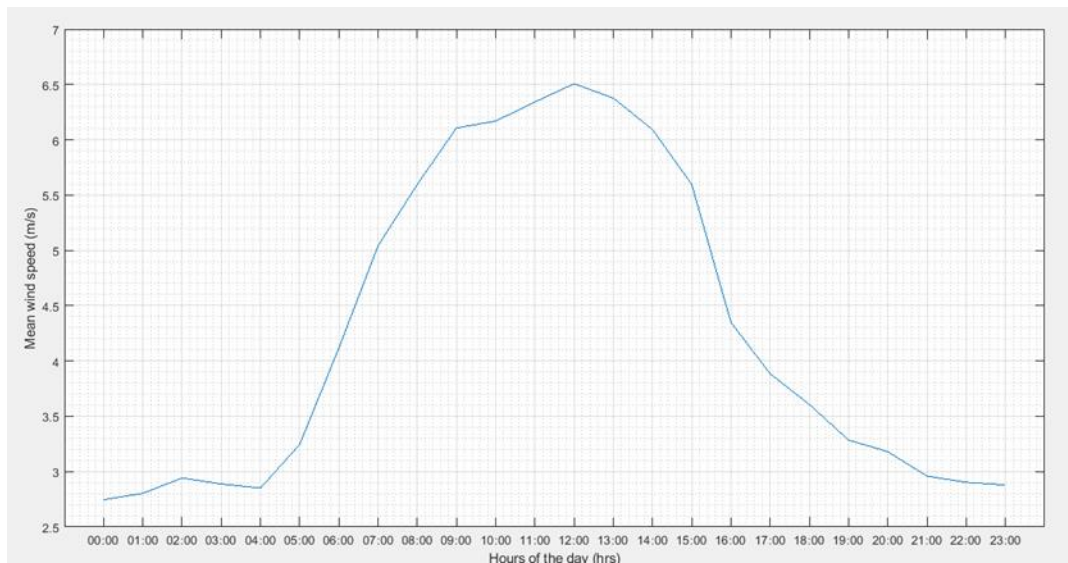


Figure 4: Diurnal mean wind speed variation for Narok weather station.

Figure 4 displays a mirror line at midday, the curve is almost symmetric about the noon hour where the maximum mean wind speed of about 6.5 m/s is registered. Mean wind speed generally ranges between 2.7 m/s and 3.0 m/s from 2100-0430 hrs. Wind speed then rises rapidly as from 0430 hrs to the maximum daily mean wind speed at around 1200 hrs. Wind speed then falls rapidly as from 1200 hrs to low wind speeds below 3.0 m/s at 2100 hrs. The profile suggests that wind regime in

Narok is correlated to the ambient temperature as was seen in section 4.1. Wind speeds are low and almost constant during low temperature hours (2100-0430hrs) while wind speeds are higher during high temperature hours (0430-2100hrs). Wind speed peaks at noon because typically, this hour is associated with highest temperature as opposed to midnight when wind speed is lowest and associated with the lowest temperature. At higher temperatures, the air density gradient steepens leading to higher wind speeds blowing over Narok region and reverse is also true. The results further suggest that domestic wind turbines, which are turbines whose rated power are <100 kW installed around Narok weather station will generate power all through the day. This is because most domestic scale wind turbines have cut-in wind speed as low as 1.5 m/s to 2.0 m/s (Oluseyi et al., 2019) and the lowest occurring hourly mean wind speed is about 2.7 m/s which occur at midnight. Most utility scale wind turbines, which are wind turbines with rated power >100 kW, on the other hand will generate power as from 0430hrs to around 2100hrs since the cut-in wind speed of most of these wind turbines ranges from 3.0 m/s to 5.0 m/s (Oluseyi et al., 2019). The suitable time for carrying out daily routine maintenance for utility scale wind turbines should be done between 2100-0430 hrs. Between these hours there is little to no wind power being generated by the turbines owing to the mean wind speeds being below the cut-in wind speeds.

4.2.2 Monthly wind speeds

Figure 5 indicates that mean wind speed distribution over the months of the year has two peaks.

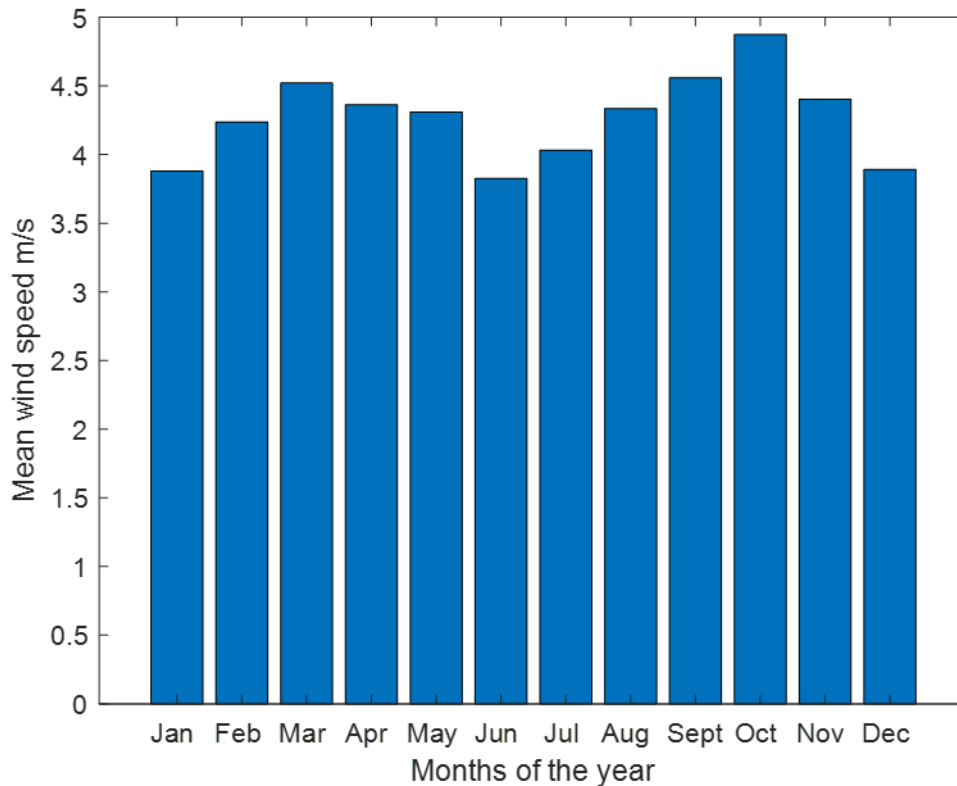


Figure 5: Mean wind speed variation over the months of the year for Narok weather station.

The peaks occur in the months of March and October. The two months are also characterized by higher temperatures than other months of the year. Therefore, the higher wind speeds might as well be attributed to the high temperatures as seen earlier. The wind regime profile in the figure is almost symmetric about the sixth month of the year. The profile is similar to that of a wave with an inverted trough; the two peaks make up a cycle (wave). This implies that the wind regime of Narok has a period of 12 months, that is, the same pattern repeats itself after every 12 months of the year. October and March are the windiest months of the year. Wind power installations in Narok are likely to generate substantial electrical power around these months of the year (Feb-May and Jul-Nov). Figure 5 also shows that all the months of the year have mean wind speeds above cut-in wind speed required for most wind turbines regardless of the scale classification of

the wind turbines. All the months have mean wind speeds above 3.5 m/s which is good enough for any meaningful power extraction from the wind by the turbines. This also implies that wind regime in Narok is classified as the gentle breeze on a wind scale, since all mean wind speeds fall in the range of 3.5 m/s to 5.0 m/s (Salvação & Guedes, 2015). It implies that, wind would have significant effect on trees and light loose flags. Flags and some trees would be swayed with their heads clearly aligning along the wind direction. Average human does not require much work to walk against such winds (Gov, 2022). The wind regime at this range does not pluck off leaves of trees and it's only capable of carrying fine dust particles with it. This explains why most dust particle deposits on outdoor surfaces around Narok station are mostly fine textured.

4.3 Mean wind speed variation with height

Mean wind speed increases with height as evident in Figure 6. The increase in mean wind velocity with height might be attributed to less physical hindrances to the flow of air as height increases.

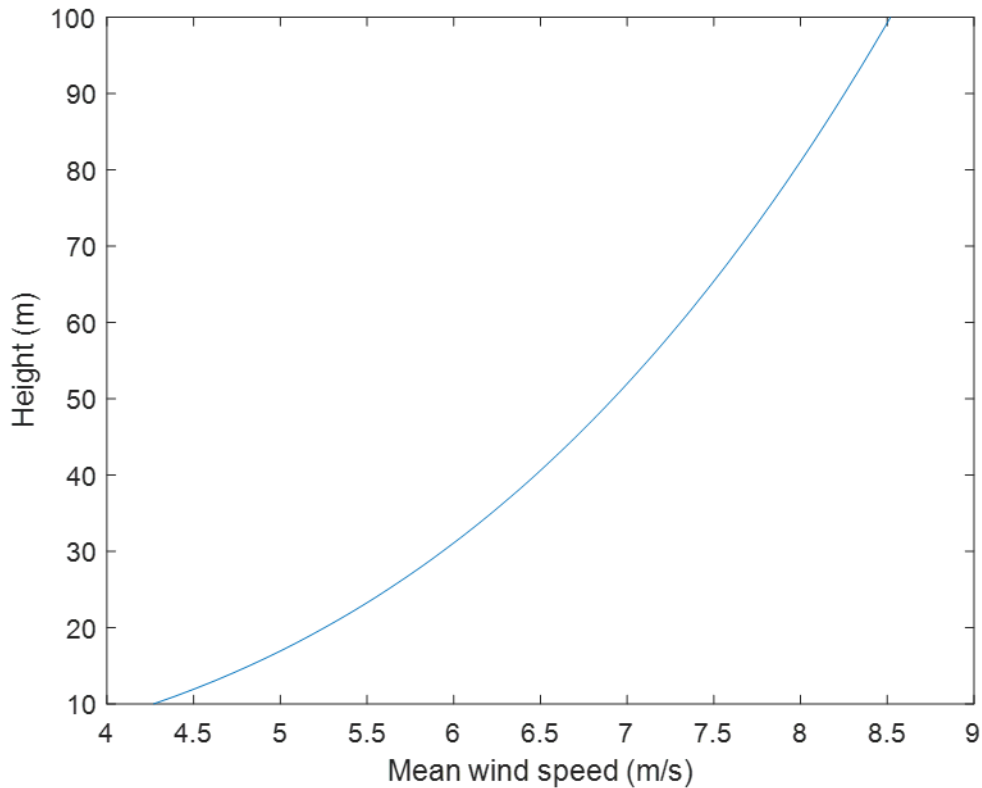


Figure 6: Mean wind variation with respect to hub height for Narok weather station

The maximum average wind speed that is likely to occur around Narok station at the maximum height (100 m) is about 8.5 m/s as observed in Figure 6. It is also evident that wind speed vertical variation follows a typical velocity profile of a fluid flowing over a surface with some degree of resistance to the flow of the fluid which is a similar observation reported by (Boming et al., 2023). Wind velocities are lowered as we approach the ground as indicated by the trend observed in the figure due to the influence of friction. The friction is greatest at the ground due to vegetations, constructions and generally rough rugged terrains. It can be deduced that hub heights should be as high as possible but less than 100 m to tap the maximum mean wind speeds occurring at heights above 10 m. The extrapolated mean wind speeds also show that Narok experiences moderate wind breeze at heights ≥ 20 m. Above 20 m height, the wind speed ranges from 5.5 m/s to 8.5 m/s

which is classified as moderate wind speeds. The mean wind speed range is classified as moderate wind breeze. Effects of moderate breeze on trees and flags are more apparent compared to light breeze discussed earlier. Moderate breeze sways almost all tree heads, even the larger ones. An average person requires much work to move against the wind. Usually, it is almost impossible to use an umbrella in this wind regime. Therefore, wind turbines having hub heights greater than 20 m, should be equipped with support structures that are able to withstand the significant pressure that would be exerted by the wind on the turbines. For instance, wind pressure is typically given by equation 33. The equation imply that wind pressure is directly proportional to the square of velocity, hence any slight increment in velocity leads to a significant increase in pressure. Since K is a location specific constant that is dependent on shape of the surface and the aerodynamics properties of the location (Begum et al., 2018).

$$P = Kv^2 \tag{4.1}$$

Where, K and v denote location specific constant and mean wind speed respectively.

4.4 Wind turbulence intensity and wind turbine stalling time

4.4.1 Daily wind turbulence intensity

Wind regime in Narok at 10 m turbine height is mostly turbulent over the entire day. This is because all turbulence intensities recorded were above 0.25 as observed in Figure 7,

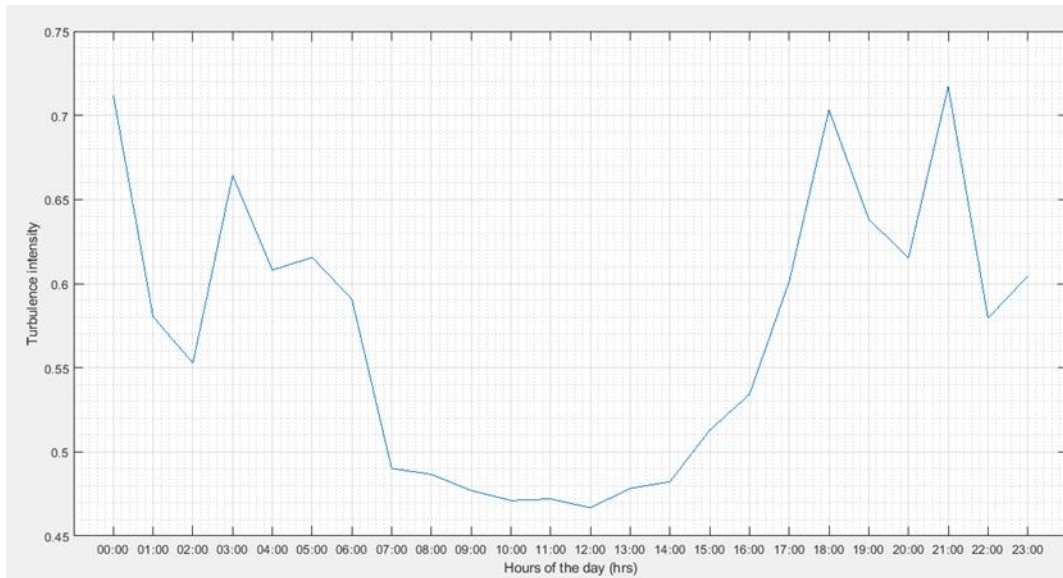


Figure 7: Wind turbulence intensity over the hours of the day for Narok weather station.

according to (John & Tony, 2015), any turbulence intensity exceeding 0.25 is considered a turbulent wind regime. High turbulence intensities observed might be arising from shear-generated turbulence due to drag. Layers of air blowing above 10 m height have faster speed than the layers of air that blows below 10 m. The upper layer is dragged by the lower layer at the boundary separating the two layers due to the difference in speed. This causes wind shear which in turn creates wind turbulence. High turbulence intensities might also be attributed to high surface roughness of the area. Narok station and its environs is generally associated with rugged terrains, vegetation and buildings which might deflect the flow of wind thus creating wind turbulences. Moreover, rugged terrains, vegetation and buildings increases the Reynolds number of the flowing mass of air to higher values exceeding 2300, which typifies fully developed turbulent wind flow. Therefore, it is reasonable to observe wind regime with high turbulent intensities around Narok. It should be noted that low wind speeds are also associated with high turbulence intensities since the turbulence intensity is indirectly proportional to the wind speed as suggested by equation 3.5 in Chapter three. The results suggest that wind turbines suitable for the area are those that are capable

of handling turbulent wind regimes. The most turbulent hours occur between 1800 to 0400 hrs. During these hours, wind turbines in operation experience a lot of mechanical stress due to gravity loading and turbulent winds. Wind turbines not designed to operate under turbulent wind regimes will most likely be stalled during these hours. Between 0700 to 1400hrs wind turbines will operate smoothly since during these hours wind regime is almost steady as indicated by the almost constant turbulence intensities between the period. The turbulence intensities are below 0.5 during the hours lying in the range 0700hrs to 1400hrs.

4.4.2 Turbulence intensity evolution over the year

Figure 8 indicates that most wind turbulence intensities are greater than 0.25 in all the months-

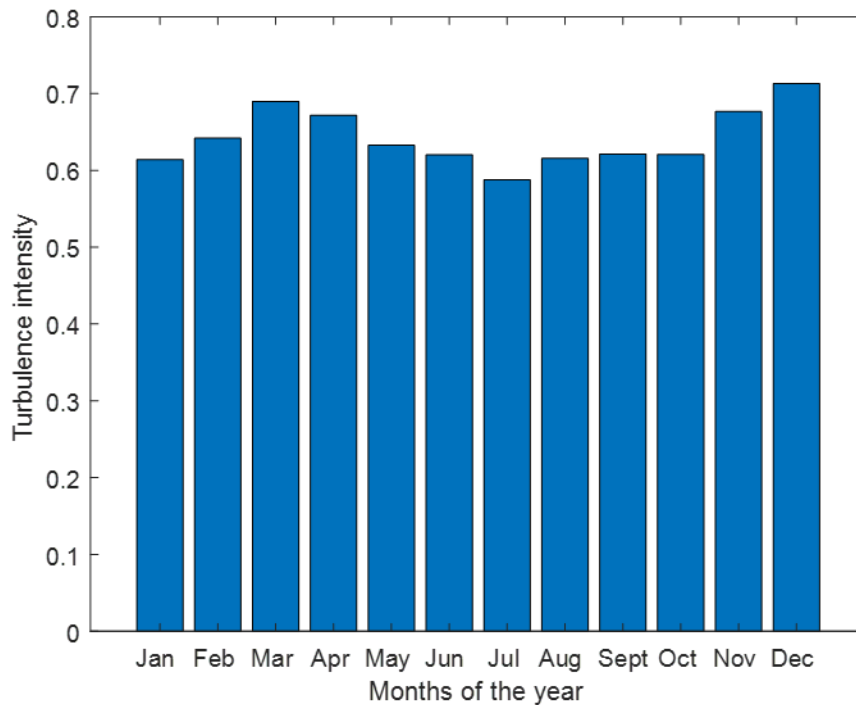


Figure 8: Turbulence intensity evolution over the year for Narok weather station.

of the year, therefore, the wind regime in Narok is turbulent all through the year. The turbulence intensities are almost constant over the year except for the months of March, April, November and December which appear to be the most turbulent months of the year as evident in Figure 8. The standard variation of the monthly turbulence intensities is ~ 0.037 which translates to coefficient of variation of $\sim 5.8\%$. This implies that the turbulence intensities are varying by only 5.8% from the mean value (about 0.64) throughout the year. Therefore, it is possible to predict the expected monthly stress related to turbulence intensity that the turbines would be subjected to using the average turbulence intensity of 0.64 as the reference. Small variation of turbulence intensities from the mean value suggests that the main cause of wind turbulence in Narok is the generally rugged terrain as suggested earlier and the terrain remains pseudo-constant for a long time. Therefore, it is logical that the turbulence intensities will also remain almost constant throughout the year. The slight variations observed in Figure 8 might be due to other characteristics inherent in the wind itself like the wind speed.

The results further affirms that wind turbines that operate within 10 m heights in Narok should be designed to handle turbulent wind regimes. From the results, it can be deduced that the most suitable time to conduct scheduled annual wind turbine maintenance is the month of December. The month is characterized by high wind turbulence intensities in addition to low wind speeds as discussed previously in section 4.2.2. These characteristics make the month of December the worst month of generating wind power as there will be a lot of damage to the wind turbine due to high wind turbulences with the least power output.

4.5 Weibull parameters

Mean and monthly Weibull parameters have been summarized in Table 3. The 'mean' below the Dec row is the scale and shape parameters over the entire sampling period. The highest scale

parameter was registered in the month of October (5.4 m/s), followed by March and September both at 5 m/s. The results indicate that during these months, wind speeds are more varied and cover a wider range than other months of the year. This wider range of wind speeds suggests that there are more occurrences of higher wind speeds compared to other months of the year, resulting to higher average wind speeds. Therefore, the average wind speed values in the months of October, March and September will be typically higher as confirmed in Figure 5. On the other hand, the least scale parameters occurred in the months of June and December hence monthly mean wind speeds are least since wind speed range coverage is least during these months.

There is little variation in shape parameters over the months of the year, shape parameter ranges from 1.4 to 1.7 and the standard deviation of the shape parameters is ~ 0.09 which corresponds to a coefficient of variation of ~ 0.059 . Therefore, there's only $\sim 5.9\%$ variation of the monthly shape parameters from the mean shape parameter. All the shape parameters are lying within the range $1 < k < 2$. This observation implies that, in all the months, there's high probability of low wind speeds occurring at 10 m height. Any mean wind speed < 5.5 m/s is considered low since moderate wind speeds starts from 5.5 m/s. This affirmation is consistent with monthly mean wind speeds seen earlier in Figure 5 which showed that there was no single month that had a mean wind speed greater than 5.5 m/s.

Table 3: Weibull Parameters c and k over the months of the year at 10 m height

Month	c (m/s)	K
Jan	4.3	1.6
Feb	4.7	1.6
Mar	5	1.4
Apr	4.8	1.4
May	4.8	1.5
Jun	4.2	1.6
Jul	4.5	1.7
Aug	4.8	1.6
Sept	5	1.6
Oct	5.4	1.6
Nov	4.8	1.4
Dec	4.2	1.4
Mean	4.7	1.5

4.6 Most probable wind speed and wind speed carrying maximum energy

Wind regime around the vicinity of Narok station has almost constant most probable wind speed-

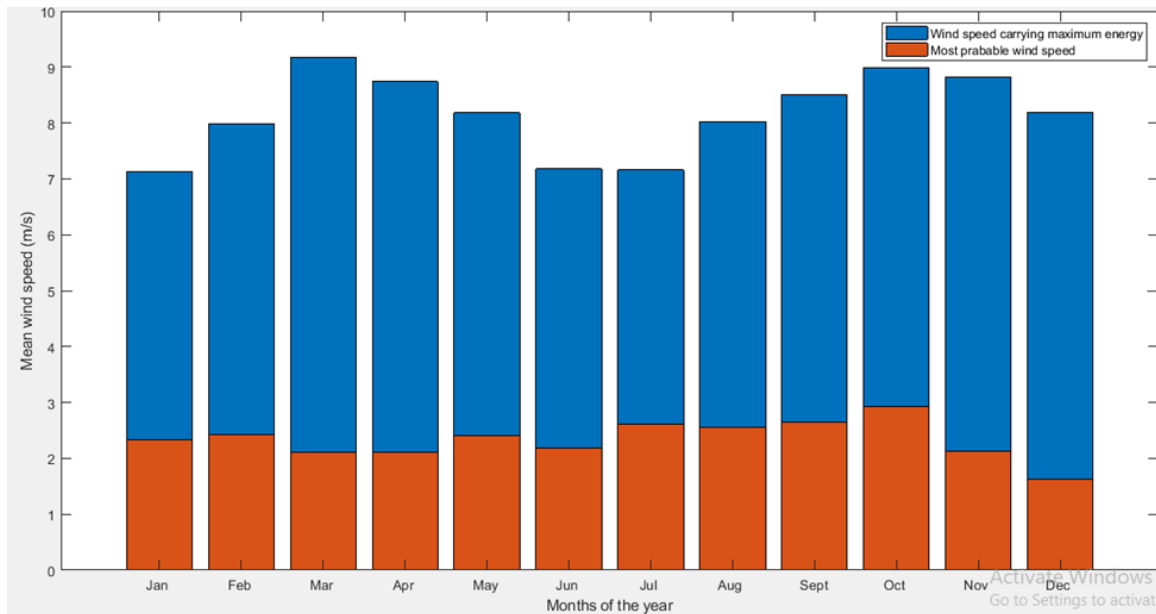


Figure 9: Most probable wind speed and wind speed carrying maximum energy for Narok weather station

as seen in Figure 9 throughout the year. The bars illustrating most probable wind speed are almost the same height which suggest an almost constant most probable wind speed. Almost all the months had most probable wind speed above 2.0 m/s. The observation suggests that, at any given month, wind blowing at approximately 2.0 m/s is likely to be observed. Therefore, throughout the year, at least wind classified as light wind breeze occur around Narok weather station. The results also imply that, wind turbines having cut-in wind speed <2.0 m/s are likely to generate power through the year without stalling due to their low threshold wind speeds. From the figure, wind speeds carrying maximum energy are always higher than most probable wind speed as expected. This category of wind speeds varied from 7.0 m/s to about 9.0 m/s at 10 m height. Therefore, wind turbines to be installed at 10 m height should have their rated wind speed within 7.0 m/s to 9.0 m/s

for maximum power extraction. Turbines' wind speed ratings should be matched with the wind speed carrying maximum energy for optimal wind power extraction as pointed out by (Djamal et al., 2017).

4.7 Measured and estimated wind speed probability and cumulative distribution densities

Figure 10 displays the comparison between the actual (histogram) and estimated (line curve)-

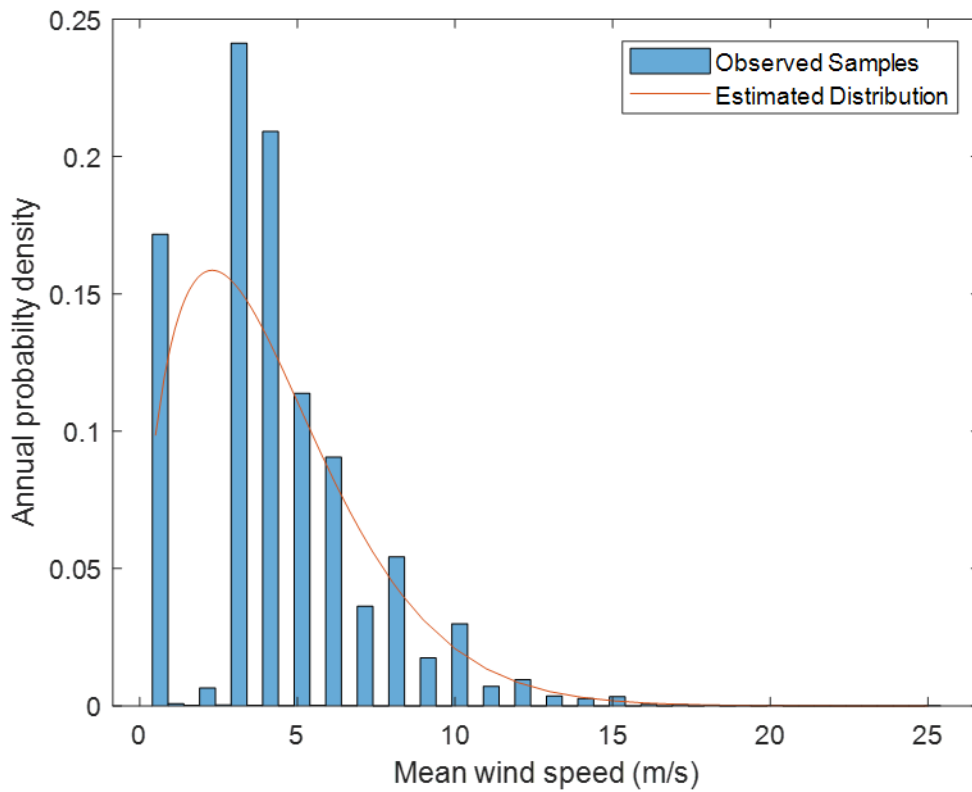


Figure 10: Mean wind speed probability distribution for Narok weather station.

wind speed probability distribution densities. The two distributions are not exactly matching; however, the profiles are generally similar. To clearly show the similarity of the Weibull PDF to the actual wind speed probability distribution, estimated and actual cumulative probability distribution curves have been presented in Figure 11.

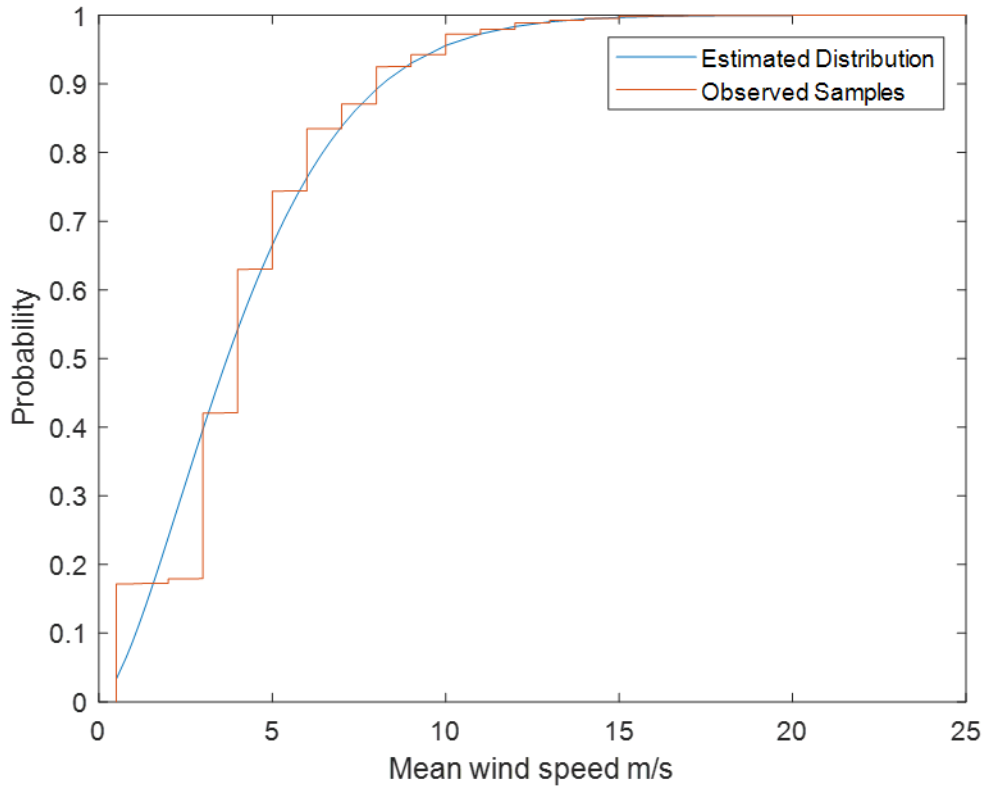


Figure 11: Mean wind speed cumulative probability distribution for Narok weather station.

The figure clearly shows the estimated cumulative probability distribution follow the same trend as the empirical counterpart. The similarity of the actual and estimated probability density distribution implies that the wind regime generally follows two parameter Weibull distribution. However, this assertion will be confirmed analytically via PDF fitness evaluation as presented in 4.8 section. Figure 11 also shows that the probability of wind speeds not exceeding 2 m/s and 3 m/s is 0.25 and 0.35 respectively. Therefore, domestic scale wind turbines (rated power <100 kW) with cut-in wind speeds ≥ 2 m/s have 75% chance of generating power while grid-tie wind turbines (rated power >100 kW) with cut-in wind speed ≥ 3 m/s have 65% chance of generating power in Narok at 10 m.

4.8 Evaluation of Weibull fitness in fitting the wind regime

The R-squared value for the fit was found to be 0.942 while RMSE registered 0.0684. Based on the goodness of fit results (R^2 and the RMSE values), Weibull distribution satisfactorily fits the wind speed regime of investigated area. The results imply that power densities estimated via Weibull PDF, will be slightly under/over estimated by about 6% in general based on the obtained error. This error should be taken into account during an actual sizing and design of wind power plant to be installed in Narok county.

4.8 Wind speed frequency spectrum

Figure 12 shows the spectral characteristics of the wind regime blowing over Narok station and-

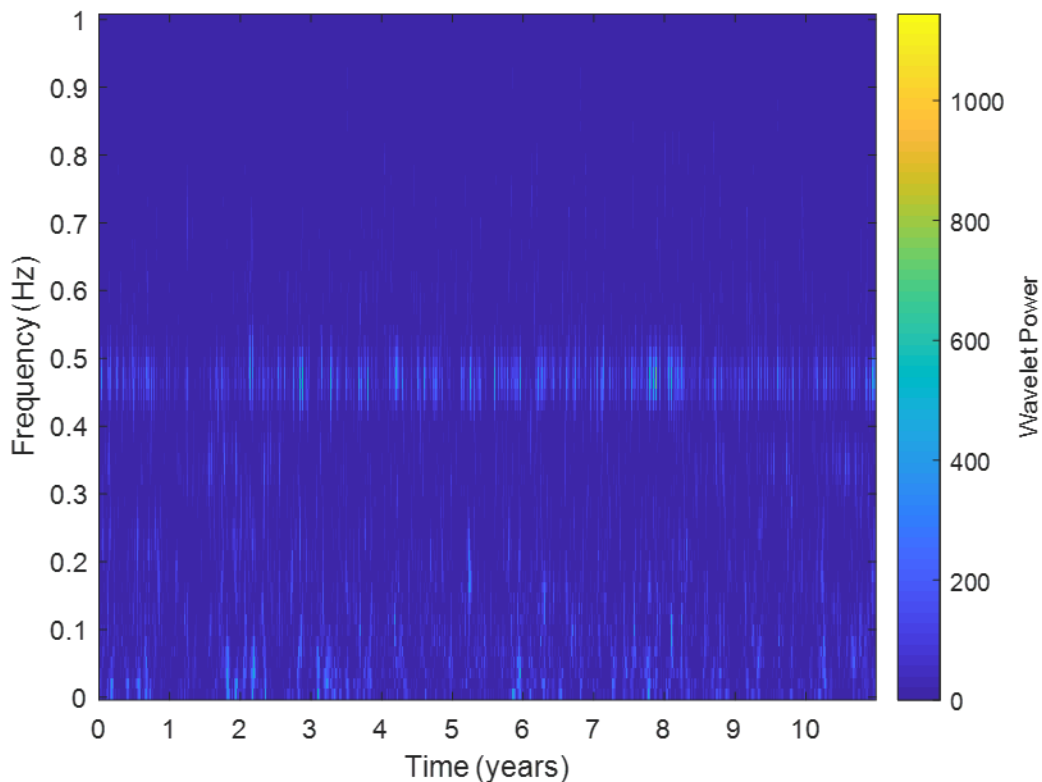


Figure 12: Time-frequency characteristics of the wind regime in Narok weather station displayed in a spectrogram.

its vicinity. The frequency spectrogram in Figure 12 shows the frequency-time distribution of the wind data recorded over a period of 11 years. The color of each point in the plot represents the power of the wind signal at that particular time and frequency. The dark blue color corresponds to the lowest power while the bright yellow color corresponds to the highest power. From the figure, there is a frequency band between 0.4 Hz and 0.5 Hz which cuts across all the years that were sampled. The band is dominated with periodic signals with a power of ~400. The band indicates persistent periodic behavior of the wind regime at the specified frequency ranges (Antonio et al., 2019). Such behavior may be attributed to consistent diurnal pattern in the wind regime, which is influenced by the periodic heating and cooling of the Earth's surface throughout the day. This is consistent with the diurnal wind variation discussed earlier where it was shown that, the wind regime corresponds to the typical daily temperature variation. Therefore, it can be concluded that daily wind behavior in Narok station is mainly influenced by atmospheric oscillations due to temperature gradient. Figure 12 can be divided into 10 divisions as shown in Figure 13.

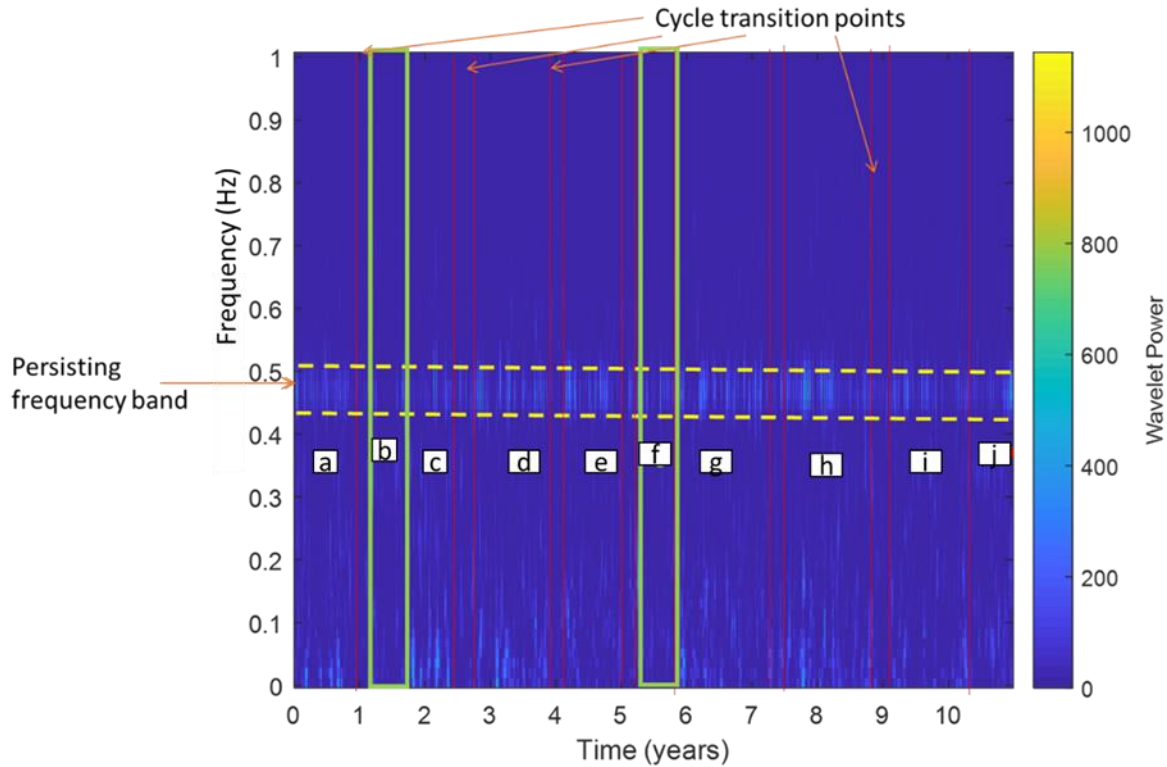


Figure 13: Time-frequency characteristics of the wind regime in Narok weather station displayed in a spectrogram (divisions of Figure 12)

Any two divisions are separated by a transition window that has little or no frequency signals at all which are indicated by the dark blue color dominating the windows. All the divisions (a-j) are having almost the same distribution of the frequencies within them except for regions b and f which have green border lines. This suggests that each region is representing a wind cycle and the similarity of the frequency shading that occur at approximately equal intervals suggests that the pattern repeats itself after every year. When you divide the 10 cycles with the 11 years you get about 0.91 cycles/year which can be approximated to 1 cycle/year. This implies that the wind regime pattern in Narok have a period of one year based on the forgoing explanation. Windows b and f appear to be very different; the two windows generally have low-power frequency signals unlike other windows. The two windows suggest an unusual wind regime behavior which might

have occurred during the time periods corresponding to the two windows. Such a behavior might have resulted from interruptions of the normal climatic weather patterns due to some unusual physical process such as interruption in atmospheric pressure and temperature gradient. The annual periodic behavior might be affirmed by zooming into any of the region in Figure 13. Figure 14 displays a magnification of region (a) in figure 13.

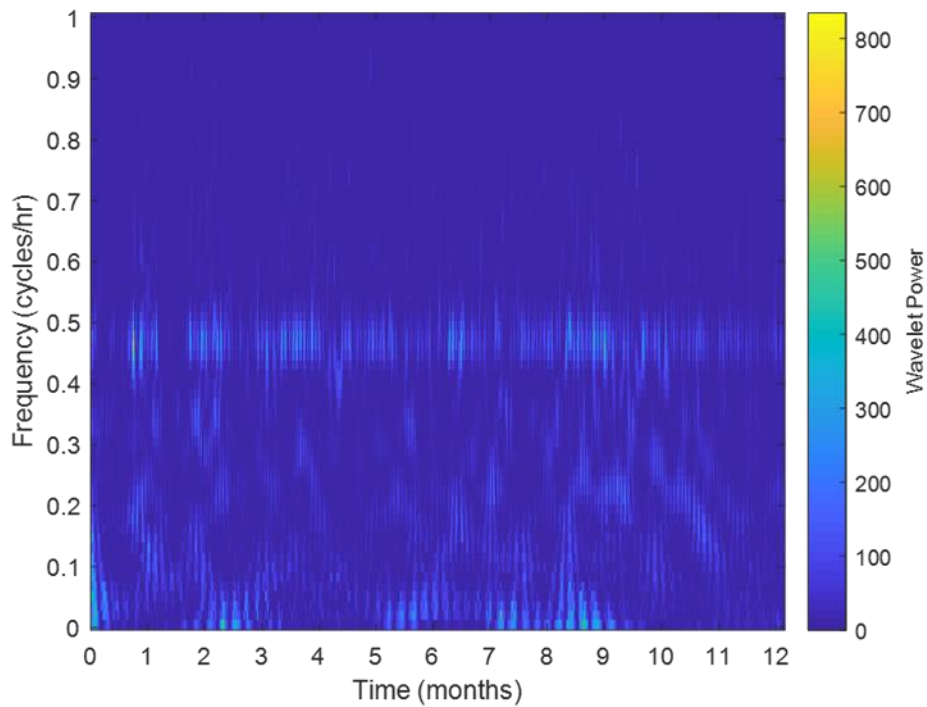


Figure 14: Time-frequency characteristics of the wind regime in Narok weather station displayed in a spectrogram, this a zoom in on region a of figure 13.

There seems to be a distribution of frequencies in the entire year with no obvious division as it was in Figure 13. The persisting frequency bands observed in figures 12 and 13 are also observed in this scenario. The absence of the transition window in the figure further affirms that a full wind long-term cycle only occurs after 1 year.

In general, the wind regime in Narok has got both diurnal and annual periodic behavior according to the observation explained above. This might be good news to potential wind power investors around the area because of an averagely consistent wind pattern. Such a pattern implies an almost predictable power generation pattern; therefore, future power plan can easily be made. For example, load matching vis a vis power generation can be made with a significant degree of confidence.

4.9 Wind Power Density

4.9.1 Monthly mean wind power density

Monthly mean wind power density has been summarized in Figure 15. Wind regime in Narok

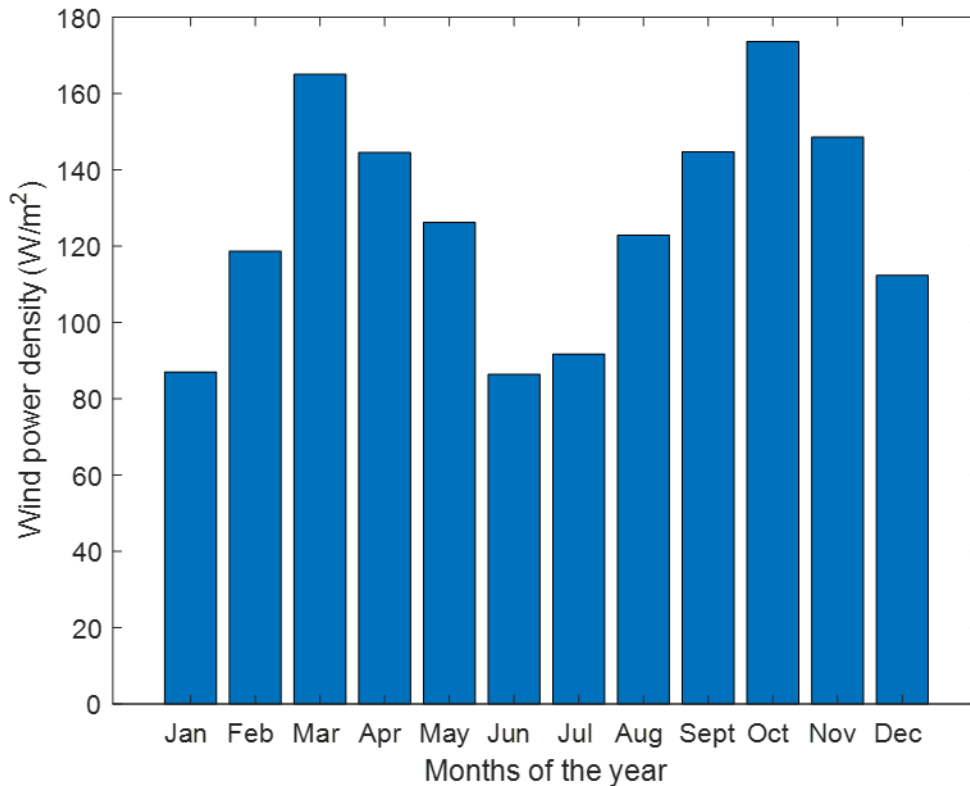


Figure 15: Mean wind power density over the months of the year for Narok weather station at 10 m height.

has got mean wind power density higher than 100 W/m^2 for nearly all the months of the year. Only in the months of January, June and July mean power densities less than 100 W/m^2 were recorded. The annual mean wind power density that was recorded is approximately 126 W/m^2 which lies between 100 W/m^2 and 160 W/m^2 . The results imply that wind power of the area belong to the class 2 wind power at 10 m anemometer height based on classification given by Heni et al. who showed that wind power density lying in the range 100 W/m^2 and 160 W/m^2 is a class 2 wind (Heni et al., 2015). Classification corresponds to wind regimes generally having mean wind speed lying in the range ≈ 4.4 to $\approx 5.1 \text{ m/s}$ and wind power densities in the range $100 - 150 \text{ W/m}^2$ which is consistent with the mean wind speed obtained during the research. Furthermore, the results are very close to the approximation by the global Wind Atlas software which showed that Narok region is characterized by wind power density of about 107 W/m^2 at 10 m height (Globalwindatlas, 2023). It is therefore not economically viable to install utility scale wind turbines at 10 m hub heights in Narok. Ideally, mean wind power density of an area should be $\geq 200 \text{ W/m}^2$ (Salvação & Guedes, 2015) to achieve economic viability of a utility scale wind power installation. However, at height greater than 10 m, the mean power density exceeds the threshold wind power density (200 W/m^2) as explained in section II.

4.9.2 Mean wind power density variation with height

Figure 16 displays an extrapolated mean wind power density at various heights. The mean wind-

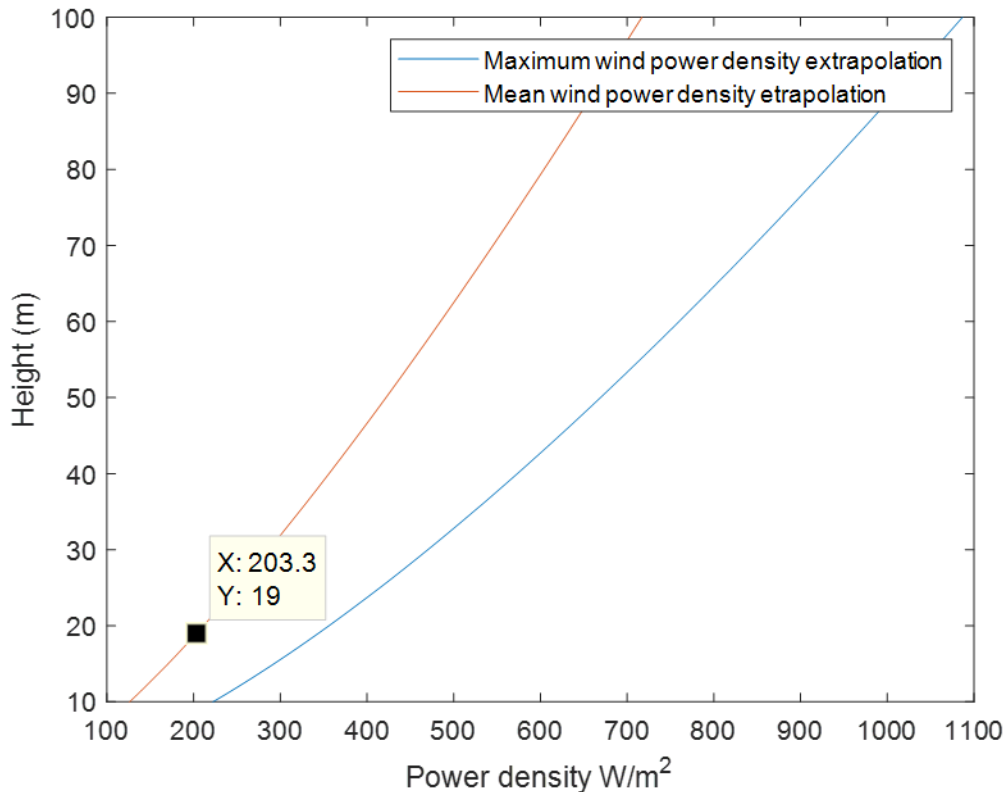


Figure 16: Wind power density variation with height extrapolated from 10 m to 100 m height.

power extrapolation is shown by the orange curve in the figure. From the curve, the mean wind power density exceeds the threshold of 200 W/m^2 which is recommended for utility scale wind power farm installation, from about 19m height. Beyond the 19 m height the classification of the wind power ranges from class 3 to class 7 depending on the hub height considered. Any area having wind regime lying within the classes mentioned is economically viable for wind power generation regardless of the scale or type of wind power installation. Based on the extrapolated mean wind power densities, utility scale wind power generation in Narok weather station and its vicinity would likely be profitable at hub heights higher than 19m. The blue curve on the other hand indicates extrapolation of the maximum wind power density likely to occur in Narok at various heights. From the curve, wind turbine power ratings at various heights can be determined.

The maximum power density occurs at 100 m height which is $\sim 1090 \text{ W}$. This implies that wind turbines with power rating of $1090\eta \text{ W}$, where η is the turbine efficiency, will capture most of the wind power at 100 m height. For example, a turbine of 0.5 efficiency will have $\sim 545 \text{ W}$ power rating. Such a turbine would operate optimally at 100 m height and below. Wind turbines designed to operate at higher turbine heights say 70 m can also operate at heights lower than 70 m say 50 m and still extract as much power as a turbine designed to work at that height (50 m) would extract. However, using higher-heights wind turbines at lower heights wouldn't be economical. That is, rate of return would be low and it would take a long time to break even.

4.9.3 Maximum possible wind power, most probable wind power and mean wind power densities comparison

Figure 17 displays comparison of maximum, mean and most probable power densities on the-

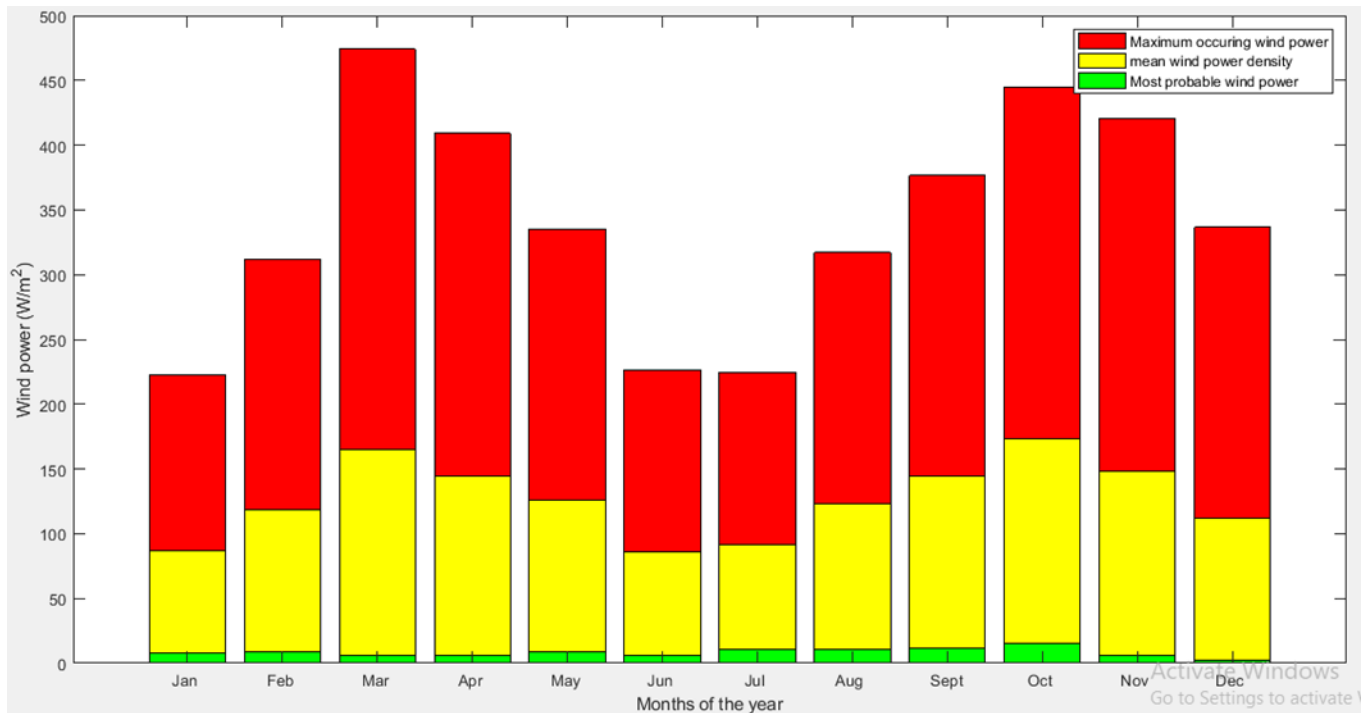


Figure 17: Comparison of the most probable, mean and maximum power densities over the year for Narok weather station at 10 m.

same axes. The arrangement of the power density profiles observed in the figure is almost similar to that one of a typical maximum, mean and minimum profiles of a well-behaved data sample. Where, the average of maximum and minimum values in a well-behaved data should be close to the mean value. Comparison of the actual mean wind power densities that were obtained against the mean densities calculated by averaging the maximum and most probable wind power densities is shown in Figure 18. Figure 18 shows a remarkable resemblance between the two mean power densities.

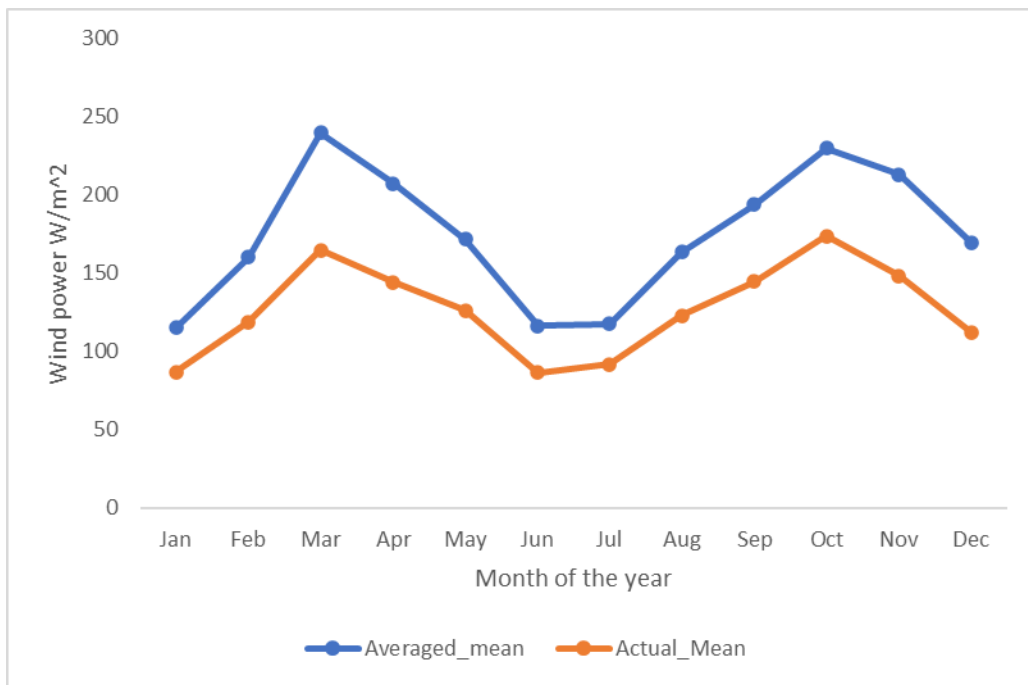


Figure 18: Comparison of the actual mean wind power densities and approximated wind power densities calculated from averaging the maximum and most-probable wind power densities

The similarity index of the two data sets in Figure 18 was found to be 0.96 based on R² analysis technique. This value translates to 96% similarity between the two data sets. This striking similarity implies that, the most probable wind power density represents the minimum wind power

density that one will most likely get from the wind regime in Narok as supported by the observation in Figure 17. Furthermore, most probable power densities correspond to most probable wind speeds which are generally ranging between 1.6 m/s to 3 m/s. In the context of diurnal wind speed behavior in Figure 4, this range of wind speeds is indeed corresponding to the lowest occurring mean wind speeds over the day. This further confirms that most probable wind power density is indeed representing the lowest wind power density in the context of Narok’s wind regime. Therefore, wind power installations whose main objective is to consistently generate a certain amount of wind power for most time of the year should have their power rating matched to most probable wind power. For example, Figure 19, subplot number 3 shows that most probable-

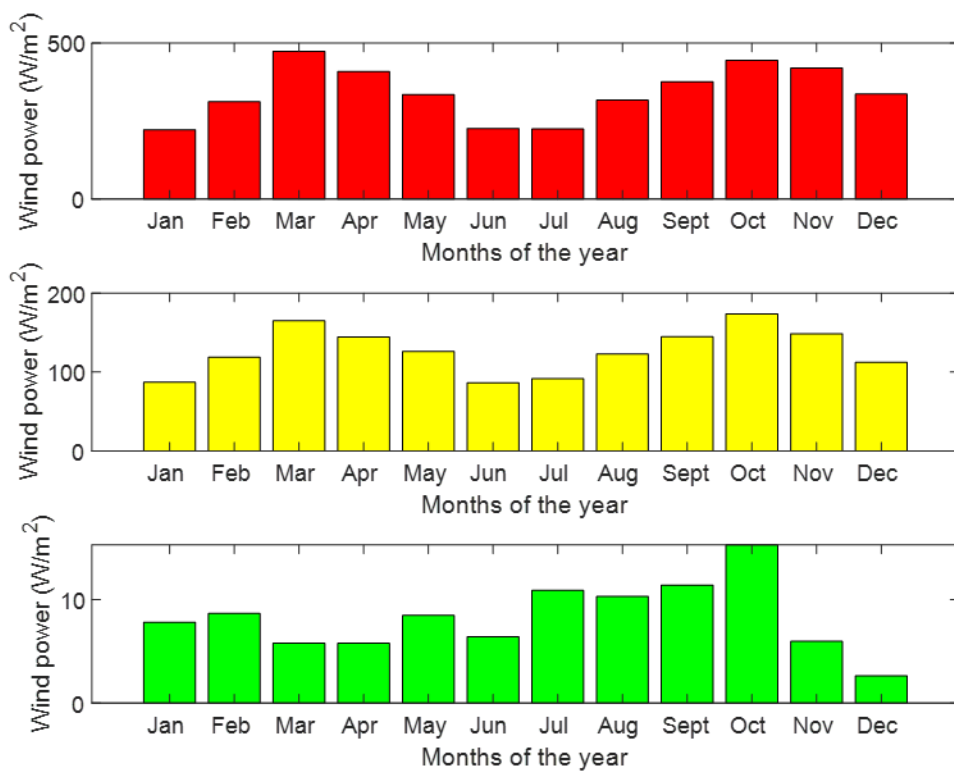


Figure 19: Sub-plots of Figure 17

power densities exceed $5 W/m^2$ in almost all the months of the year except for the month of December. Therefore, wind turbines with power rating of $\sim 5\eta W/m^2$ will consistently generate constant power for most time of the year. Note that Figure 19 is just a decomposition of Figure 17, this was done for the sake of clarity.

In cases where the main objective of an installation is to generate as much power as possible, the design and wind power farm sizing should be based on the mean WPD coupled with the maximum WPD displayed in the Figure 17. Maximum power density occurs in the month of march at $\sim 475 W/m^2$. To extract most of the available power throughout the year at 10 m height, wind turbines of $\sim 475\eta W/m^2$. power rating should be used. The trends in all the plots also suggest that most suitable time for wind power installation (in Narok) maintenance is at the start and end of the year with a short window at middle of the year. The mentioned periods are characterized by low power densities hence shutting down a wind power plant wouldn't do much harm economically and even in terms of total wattage withdrawn from the national grid.

CHAPTER FIVE

Conclusions and Recommendations

5.1 Conclusions

Wind regime in Narok is predominantly blowing from the East direction. The directions of the wind regime lie in the upper two quadrants of the Windrose chart bound by East and West directions. The wind is characterized by a turbulence intensity of about 0.6 which is above 0.25. Therefore, the wind regime is classified as turbulent wind. The annual mean wind speed of the wind regime occurring in Narok is about 4.3 m/s. The wind regime blowing over Narok at 10 m height can be classified as gentle breeze since most wind speed lie in the range 3.5 m/s to 5 m/s. The wind regime in Narok generally follows Weibull probability distribution. The function describes the wind regime with an average accuracy of 0.94 and 0.0684 based of R^2 and RMSE best of fit analysis criteria. The wind regime is characterized by both diurnal and yearly cycle periods, that is, the wind pattern repeats itself after every one day and 1 year respectively. The available wind power density at 10 m height was found to be 126 W/m² which is classified as class II wind power. The category of Narok wind power ranges from class II to class VII depending on the hub height. Therefore, Narok is a viable region for wind power extraction for utility scale wind power installations as from the height of 19 m. For domestic scale wind power generation on the other is viable throughout as from 10 m height.

5.2 Recommendations

The study adopted wind shear constant value for Narok as 0.3 based on physical observations of the area and published research papers in peer reviewed journals. Further investigations should be conducted to ascertain the true value of the shear constant for Narok which as it stands can only be approximated.

5.3 Appendices

This section consists of all the flowcharts that represent the logic that was used in implementing various methods in MATLAB environment. All the symbols bear their meaning as declared in list symbols and abbreviation of symbols unless stated otherwise in further definitions given in statements next to the figure itself.

Figures 20 and 21 combined represents the logic that was followed to filter wind speed data as explained in section 3.1. In the two figures, i denotes the value or magnitude of each data cell while N represents the total number of data points. The abbreviation ‘Cal’ means to calculate.

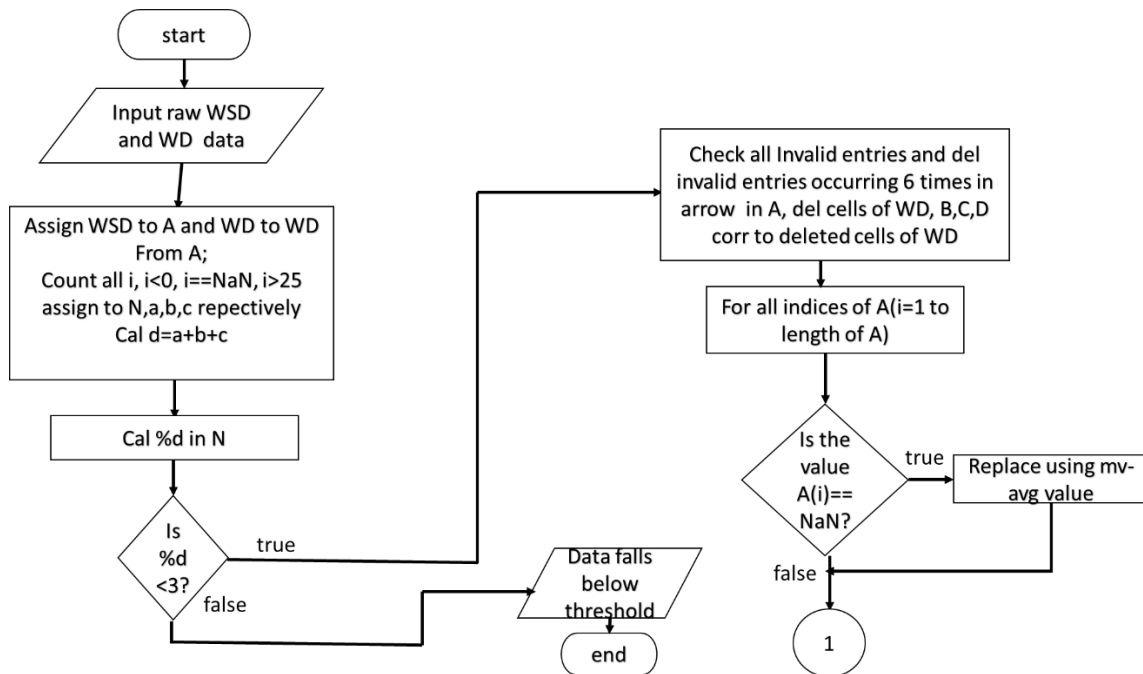


Figure 20: Flowchart for filtering wind speed data part I

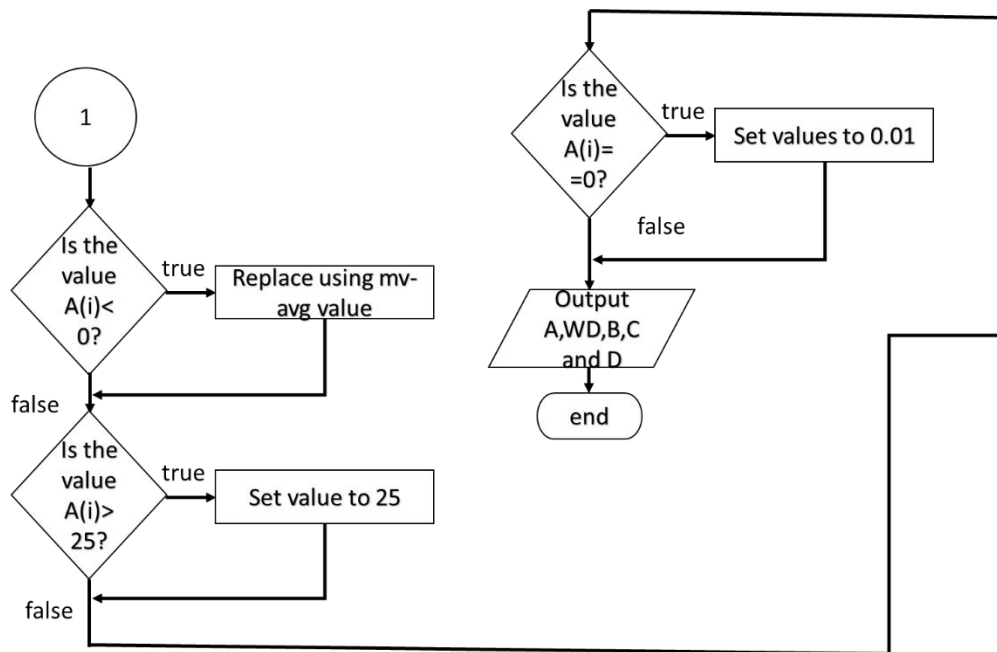


Figure21: Flowchart for filtering wind speed data part II

Figures 22 and 23 summarize the logic that were employed in filtering wind direction data. All symbols bear their normal meaning as earlier defined.

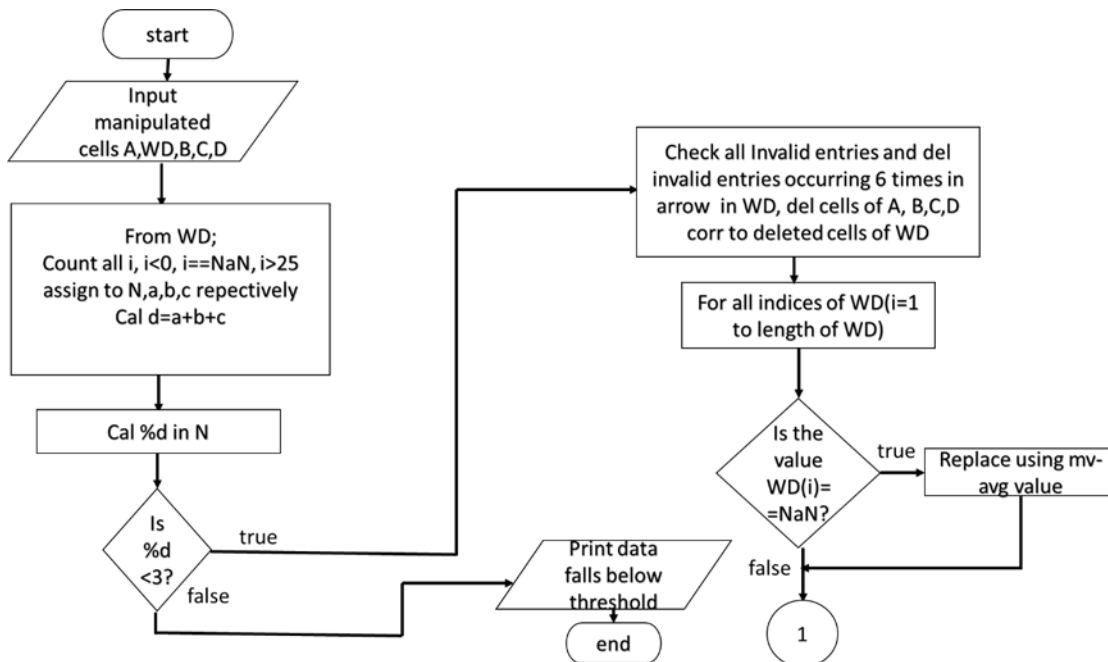


Figure 22: Flowchart for filtering wind direction data part I

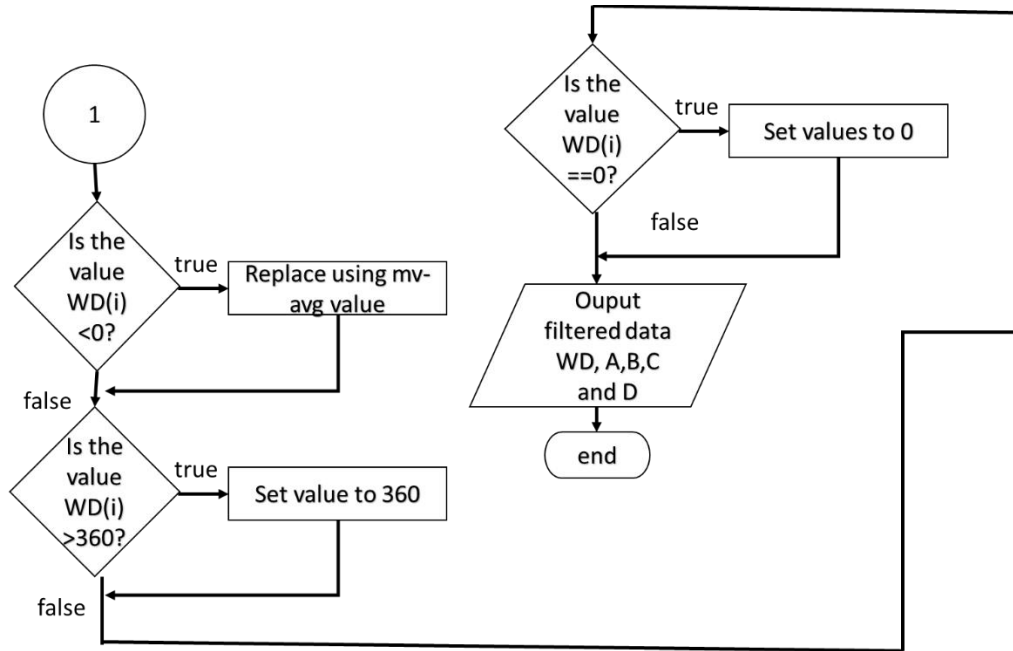


Figure 23: Flowchart for filtering wind direction data part II

Figure 24 is the flowchart that corresponds to the method explained in section 3.2 Chapter Three.

The symbol freq-dist denotes frequency distribution.

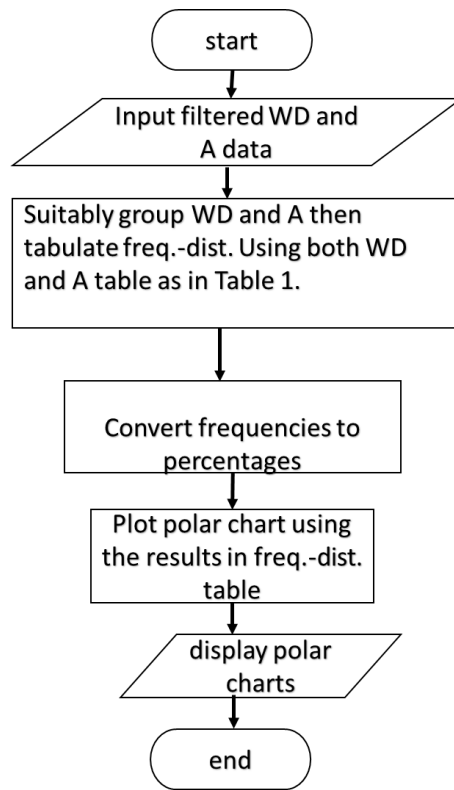


Figure 24: Flowchart showing the logic for tabulating WSD & WDD and plotting polar chart

Figures 25 and 26 correspond to method in section 3.3, std in the figure represents standard deviation.

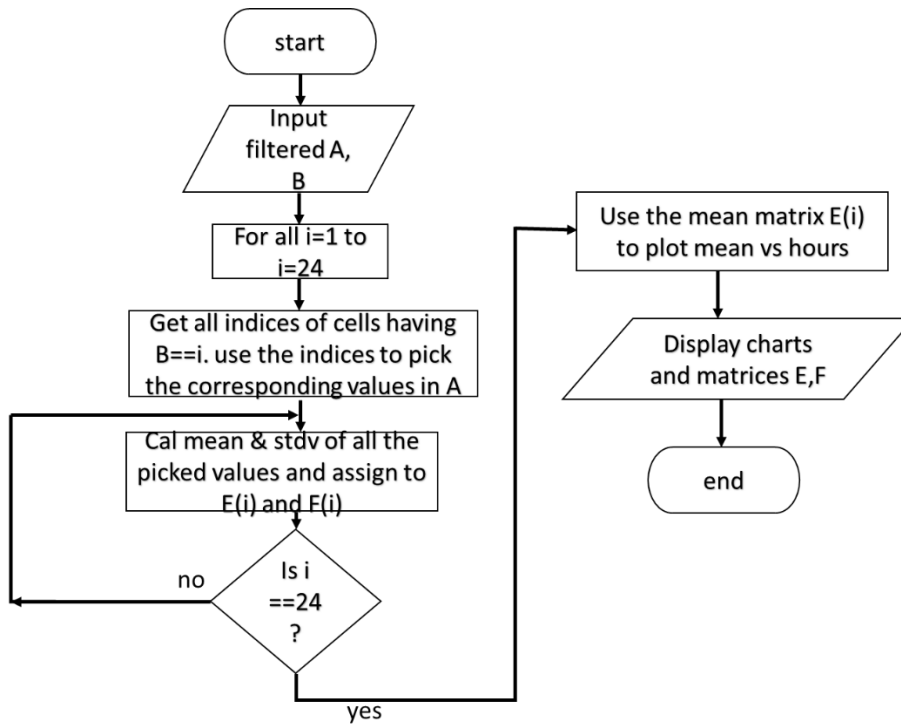


Figure 25: Flowchart for determining hourly mean wind speed and standard deviation

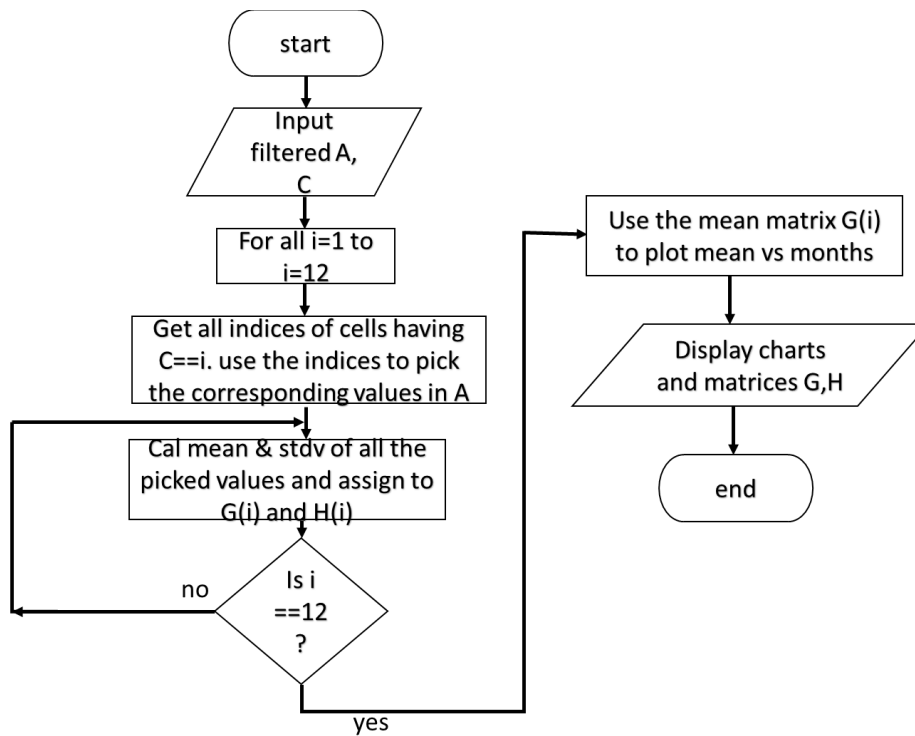


Figure 26: Flowchart for calculating monthly and annual mean wind speed and standard deviation

Figures 27 and 28 correspond to methods in 3.7 and 3.8 respectively. The abbreviations prob-den and cum-prob-den means probability density and cumulative probability density respectively.

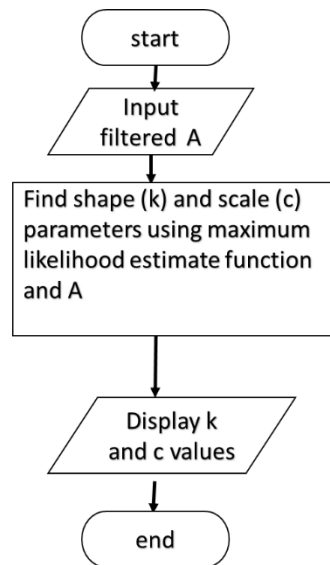


Figure 27: Flowchart for calculating algorithm parameters k and c

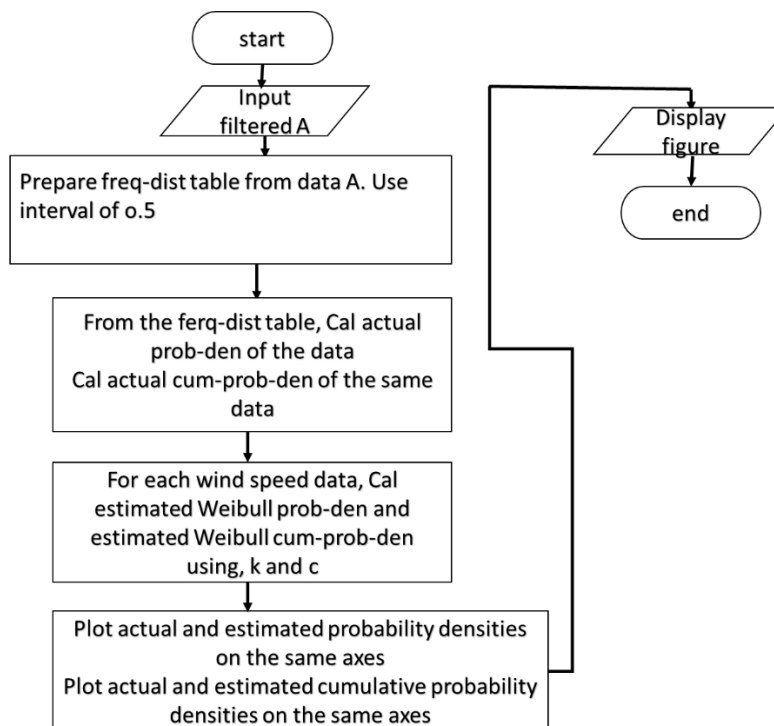


Figure 28: Flowchart showing steps for computing estimated and measured probability and cumulative densities of Weibull distribution.

Figure 29 is the flowchart used for spectral analysis; it corresponds to method in section 3.11. The symbols and cwt and Morlet stand for continuous wavelet transform and Morlet wavelet functions. It should be noted that both functions are already built in MATLAB.

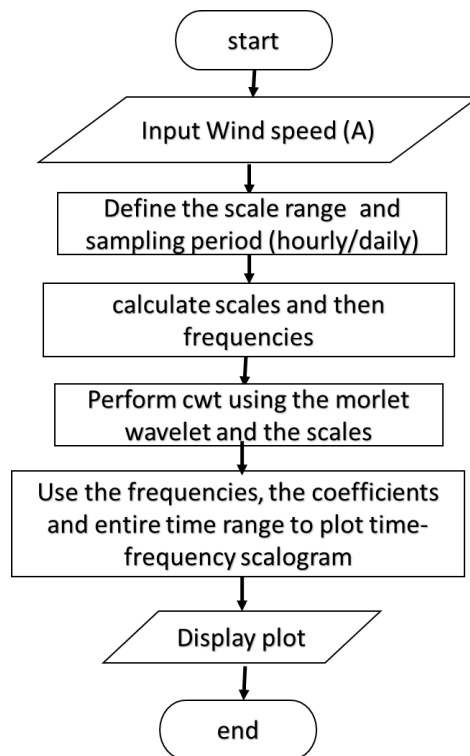


Figure 29: Flowchart showing the algorithm that was used for spectral analysis of WSD

References

- Abdoul A., David T., Nsouandele J., Inouss M., Reuben M. & Patrice E. A. (2023). Influence of Weibull parameters on the estimation of wind energy potential. *Sustainable Energy Research*, 5, 10.
- Agency, I. E. (2021). *Global Energy Outlook Report*.
- Ahmed A., Azam M. & Adrian S. (2018). Cluster sampling filters for non-gaussian data assimilation. *Atmosphere*, 9, 213. doi:10.3390/atmos9060213
- Ali K. R., Ahmed B. K., & Saif F. Y. (2020). Determination of wind shear coefficients and conditions of atmospheric stability for three Iraqi sites. *3rd International Conference on Sustainable Engineering Techniques*, (p. 881).
- Amos O. O., Anthony J. R. & Wafula J. M. (2020). A system dynamics model of technology and society: In the context of a developing nation. *International Journal of System Dynamics Applications*, 9(2), 22. doi:10.4018/IJSDA.2020040103
- Antonio J. Z., Alejandro C., Francisco G. M., Alfredo A. and Francisco M. and Agugliaro O. (2019). Wind missing data arrangement using wavelet based techniques for getting maximum likelihood. *Energy Conversion and Management*, 185, 552-561.
- Antonio J. Z., Alejandro C. P., Francisco G. M., Alfredo A. & Francisco M. A. (2019). Wind missing data arrangement using wavelet based techniques for getting maximum likelihood. *Energy Conversion and Management*, 185, 552-561.
- Asaad M., Ahmad F., Alam M. S., & Das G. (2017). Automation of the Grid: Indian Initiatives. *2017 IEEE International Conference on Technological Advancements in Power and Energy (TAP Energy)*. Delhi, India.
- Authority, E. a. (2021, 11 4th). *Energy and Petroleum Statistics*. Nairobi: Kenyan government press. Retrieved 4 2nd, 2022, from <https://cleantechnica.com/author/remeredzaijosephkuhudzai/>
- Authoriy, E. a. (2020, January 1st). *EPRA Renewable Energy*. (EPRA, Kenya) Retrieved 5 2nd, 2022, from <https://renewableenergy.go.ke/technologies/wind-energy/>
- Begum Y. D., Yeşim T., & Ümit G. (2018). Evaluation of offshore wind turbine tower dynamics with numerical analysis. *Advances in Civil Engineering*, 11.
- Boming L., Xin M., Jianping G., Hui L., , Shikuan J., Yingying M., & Wei G. (2023). Estimating hub-height wind speed based on a machine learning algorithm: implications for wind energy assessments. *Atmos. Chem. Phys*, 23, 3189-3193.
- Chemengich S. J. & Masara D. O. (2022). The state of renewable energy in Kenya with a focus on the future of hydropower. *African Environmental Review*, 5(1), 246-260.
- Cherinet S. A., Kassahun T. B., Desalegn Y. A. & Zerihun T. D. (2020). Multiple criteria application in determining wind power potential: A case study of Adama Zuria woreda, Ethiopia. *Scientific African*, 14, 01045.

- Cheruiyot W. K., Tonui J. K. & Limo S. C. (2016). Assessment of wind energy potential at Kesses region-Kenya based on Weibull parameters. *International Journal of Advanced Research*, 4(7), 641-648.
- Choge, D. (2015). Analysis of wind and solar energy potential in Eldoret, Kenya. *Journal of Energy Technologies and Policy*, 5(2).
- Community, E. A. (2016). *The EAC renewable energy and efficiency status report*. REN21.
- Daoudi M., Abdelaziz A. M., Mohammed E. K., & Elkhouzai E. (2019). Analysis of wind speed data and wind energy potential using Weibull distribution in Zagora, Morocco. *International Journal of Renewable Energy Development*, 8(3), 267-273.
- Devasani S. K. R., Vodnala S. & Singarapu D. (2021). A comprehensive review on performance, combustion and emissions of ternary and quaternary biodiesel/diesel blends. *Environ Sci Pollut Res*. doi:<https://doi.org/10.1007/s11356-021-17504-4>
- Dida, G.O., Lutta P. O. & Abuom P. O. (2022). Factors predisposing women and children to indoor air pollution in rural villages, Western Kenya. *Arch Public Health*, 80, 46. doi:<https://doi.org/10.1186/s13690-022-00791-9>
- Djamal H. D., Nurhayati R., Mohd F. Z. & Syariful S. S. (2017). Evaluation of wind energy potential as a power generation source in Chad. *International Journal of Rotating Machinery*, 10.
- Eleonora G., Audrius S., Serhat S. & Tahir C. A. (2014). Statistical and continuous wavelet analysis of wind speed data in Mardin-Turkey. *Ninth International Conference on Ecological Vehicles and Renewable Energies (EVER)*.
- Elsayed M. (2010). An overview of wavelet analysis and its application to ocean wind waves. : *Journal of Coastal Research*, 263, 535-540.
- Francisco B., César Á. C. & Sebastián R. (n.d.). Methodologies Used in the extrapolation of wind speed data at different heights and its impact in the wind energy resource and assessment in a region. *intechopen*.
- Globalwindatlas*. (2023). (Global windatlas) Retrieved July 23, 2023, from <https://globalwindatlas.info/en/area/Kenya/Narok>
- Gov, A. (2022, may 12). *Bureau of Meteorology*. Retrieved June 11, 2023, from <http://www.bom.gov.au/marine/knowledge-centre/reference/wind.shtml>
- Grinsted A., Moore J. C & Jevrejeva S. (2004). Application of the cross wavelet transform and wavelet coherence to geophysical time series. *Nonlinear Processes in Geophysics*, 11, 561-566.
- Gugliani G. K., Sarkar A., Mandal S. & Agrawa V. (2017). Location wise comparison of mixture distributions for assessment of wind power potential: A parametric study. *International Journal of Green Energy*, 1543-5083. doi:DOI: 10.1080/15435075.2017.1327865

- Hanbo Z., Wufeng H., Junhui Z., Jiefeng L., Yiyi Z., Zhen S. & Chaohai Z. (2022). A novel falling model for wind speed probability distribution of wind farms. *Renewable energy*, 184, 91-99.
- Heni K. S., Khamees A. B. & Raja O. H. (2015). Wind power density estimation in the middle of Iraq “Karbala Site”. *world*.
- Ibrahim K. R., Hilda C. & Peter K. M. (2024). Renewable energy status and uptake in Kenya. *Energy Strategy Reviews*, 54, 101453.
- Ivana P., Zuzana S. & Mária M. (2017). Application of four probability distributions for wind speed modeling. *Procedia Engineering*, 192, 713-718.
- Jaramilo O. A. & Borja M. A. (2004). Windspeed analysis in La Ventosa, Mexico: A bimodal probability distribution case. *Renewable Energy*, 29, 1613-1630.
- John T. & Tony W. (2015). *Renewable energy resources*. London: Routledge.
- John T. & Tony W. (2015). Wind resource. In *Renewable Energy Resources* (p. 257). New York: Routledge.
- Justus N. M, David W. W. & Joseph K. (2019). Analysis of wind resource potential for small-scale wind turbine performance in Kiseveni, Kenya. *International Journal of High Energy Physics*, 6(1), 17-29.
- Kalam A., Mohammad R., Pobitra H. & Sutariya J. (2019). Assessment of wind energy prospect by Weibull distribution for prospective wind sites in Australia. *2nd International Conference on Energy and Power, ICEP2018, 13–15 December 2018, Sydney, Australia*. Sydney.
- Kamau J. N., Kinyua R. & Gathua J. K. (2011). An investigation of the utility scale wind energy for North-Eastern Kenya region. *JAGST*, 2, 13.
- Kengne S. E. B., Kanmogne A. & Meva’a L. (2020). Sustainable Energy through wind speed and power density analysis in Ambam, south region of Cameroon. *Frontiers in Energy Research*, 8, 176.
- Kennedy M., Kamau J. N., Wafula W. D., Otieno S. C., Joseph N. M. & Joseph K. G. (2023). Wind and solar resource complementarity and its viability in wind/PV hybrid energy systems in Machakos, Kenya. *Scientific Africn*, 20.
- kfw, giz, Irena & Federal Ministry of Economic Cooperation and Development. (2021). *The Renewable Energy Transition in Africa*.
- Kiche J., Oscar N. & George O. (2019). On Generalized Gamma distribution and its application to survival. *International Journal of Statistics and Probability*, 8(5).
- Kwamboka J. O., Kamau J.N, Saoke C. O., Ndeda J. O. & Maina A. W. (2018). Analysis of the wind Energy characteristics and potential on the hilly terrain of Manga, Nyamira County, Kenya. *International Journal of Innovative Science and Research Technology*, 3(3), 34-35.

- Lizica S. P., Spiru P. & Ion v. (2019). Investigation of wind power density distribution using Rayleigh probability density function. *emergy precidia*, 175, 1546-1552.
- Ma, D. (2017, 8 18). *Dan Ma*. (Dan Ma) Retrieved 6 7, 2022, from <https://actuarialmodelingtopics.wordpress.com/2017/08/18/mixing-probability-distributions/>
- Maguta J. K., Nzengya D. M., Mutisya C., & Wairimu J. (2021). Building capacity to cope with climate change-induced resource-based conflicts among grassroots communities in Kenya. In *African Handbook of Climate Change Adaptation* (pp. 2611–2630). Springer.cham. doi:https://doi.org/10.1007/978-3-030-45106-6_131
- Marta W. & Adam K. (2022). Application of continuous wavelet transform and artificial neural network for automatic radar signal recognition. *Sensors*, 22(19), 30-36.
- Mekalathur B. H. K., Saravanan B., Sanjeevikumar P. & Jens B. H. (2019). Wind energy potential assessment by Weibull parameter estimation using multiverse optimization method: A case study of Tirumala region in India. *Energies*, 12(11), 2158.
- Mohamed B., Ali H., Youness E. M., Ahmed S., Abderrahman M., Abderrahman E. K., Saleh M., Anton Z. & Badre B. (2023). Analysis and comparison of wind potential by estimating the Weibull distribution function: Application to wind farm in the northern of Morocco. *Sustainability*, 15(20), 20-22.
- Mohammed T., Rogers K., & Paul K. E. (2021). A comprehensive review of energy scenario and sustainable energy in Kenya. *Fuel Communications*, 7, 100015. doi:<https://doi.org/10.1016/j.jfueco.2021.100015>
- Muhammad S., Saif R., Imran S., Shafiqur R., Shamim K. & Zia I. (2020). Comparison of Weibull and Gaussian mixture models for wind speed data analysis. *Int. J. Econ. Environ. Geol*, 11(1), 10-16.
- Muhammad S., Tauseef A., Syed A. G., Muhammad M. B., Syed M. S. R. & Syed U. R. (2021). Application of five continuous distributions and evaluation of wind potential at five stations using normal distribution. *Energy Exploration & Exploitation*, 39(6), 2214-2239.
- Munir A. E. & Mustafa K. (2018). Comparison of optimum spline-based probability density functions to parametric distributions for the Wwind speed data in terms of annual energy production. *Energies*.
- Nawel A., Sidi M. B. & Houdayfa O. (2018). Deep assessment of wind speed distribution models: A case study of four sites in Algerial. *Energy Conversion and Management*, 155, 78-90.
- Nil A., Ulku E. & Hasan D. Y. (2020). Optimum method for determining Weibull distribution parameters Used in wind energy estimation. *Pak.j.stat.oper.res*, 16(4), 635-648.
- Nyasani E. I., Mathew M., Mukuru S. A., Muhorakeye L. & Douglas N. (2018). Wind energy assesment as a potential alternative in Kisumu city, Kenya. *World Journal of Engineering Research and Technology*, 4(4), 75-104.

- Oluseyi O. A., Olorunfemi O., & Ahmed V. (2019). On the need for the development of low wind speed turbine generator system. *International Conference on Energy and Sustainable Environment*.
- Ongaki L. N., Christopher M. M. & Kerongo J. (2021). Evaluation of the technical wind energy potential of Kisii region based on the Weibull and Rayleigh distribution models. *Journal of Energy*, 17.
- Otieno O, K., Troon J. B. & Samuel M. N. (2021). Fitting wind speed to a 3-parameter distribution using maximum likelihood technique. *International Journal of Statistical Distributions and Applications*, 7(1), 1-6. doi:doi: 10.11648/j.ijstd.20210701.11
- Pritha, B. (2020). *Scribbr*. (Scribbr) Retrieved 5 2022, 28, from <https://www.scribbr.com/statistics/normal-distribution/>
- Rajapaksha K. G. & Kanthi P. (2016). Wind speed analysis and energy calculation based on mixture distributions in Narrakalliya, Srilanka. *J.Natn. Sci. Foundation Sri Lanka*, 44(4), 409-416.
- Salvação N. & Guedes S. C. (2015). Offshore wind energy assessment for the Iberian coast with a regional atmospheric model. *Renewable Energies Offshore*.
- Shaima' B. Y. & Iden H. K. (2021). Estimation of the parameters by using non-Bayesian in modified Weibull extension distribution. *IMDC-IST*.
- Shu Z. R. & Mike J. (2021). Estimation of Weibull parameters for wind energy analysis across the UK. *Journal of Renewable and Sustainable Energy*, 023303, 13.
- Stefano B., Guido B. & Giuseppe P. (2022). Thunderstorm-induced mean wind velocities and accelerations through the continuous wavelet transform. *Journal of Wind Engineering and Industrial Aerodynamics*, 221, 104886.
- Suphi S. O. & Cecilia F. (2018). Environmental factors affecting Hydrogen production from *Chlamydomonas reinhardtii*. In *Microalgal Hydrogen Production: Achievements and Perspectives* (pp. 265-298). Royal Society of Chemistry. doi:<https://doi.org/10.1039/9781849737128-00265>
- Tian P. C., Feng J. L., Hong H. K. & Ming C. H. (2017). Oscillation characteristic study of wind speed, global solar radiation and temperature analysis. *Applied Energy*, 190, 650-657.
- weatherspark.com*. (n.d.). (weatherspark) Retrieved 7 21, 2023, from <https://weatherspark.com/y/148690/Average-Weather-at-Narok-Kenya-Year-Round>
- Younes E. K. , Mohammed S., Nacer E. E. & Kadri E. (2019). Evaluation of wind energy potential and trends in Morocco. *Heliyon*, e01830.